

**Transit Cooperative Research Program**  
Sponsored by the Federal Transit Administration  
**RESEARCH RESULTS DIGEST**

June 1998--Number 26

Subject Area: VI Public Transit

Responsible Senior Program Officer: Christopher W Jenks

### **Rail Corrugation Mitigation in Transit**

*This TCRP Digest summarizes the findings from TCRP [Project D-1](#), "Rail Corrugation Mitigation In Transit, " conducted by the Association of American Railroads' Transportation Technology Center, Inc This digest was prepared by Barrie Brickle on the basis of work performed by John Elkins, Stuart Grassie, and Stephen Handal at the Transportation Technology Center*

#### **INTRODUCTION**

This digest identifies and classifies various types of transit rail corrugation and offers possible mitigation measures for each. The body of the digest summarizes the work performed and the resultant findings. More detailed information is provided in the appendixes. This information will be of particular use to track engineers and others involved in mitigating rail corrugation.

The corrugation of rails is a problem that has occurred on railroad systems worldwide since the inception of railroads; it continues to be a significant difficulty today. Transit systems in particular appear to suffer from corrugation. The resulting vibration and noise has become an increasing nuisance in urban areas. The principal means of control by transit systems is the removal of corrugations by rail grinding-an operation that costs the railroad industry worldwide an estimated \$100 million (U. S. dollars) each year.

Corrugations on transit systems could be associated with the acceleration and braking rates at which transit vehicles operate. These rates are comparatively higher than most mainline rail operations and, in particular, freight railroad systems. Transit vehicles usually have more of their axles driven than other railroad systems.

The literature on corrugations is vast; a large volume of research has been performed regarding the subject. As a result of this research and supporting experimental work, various theories have been proposed to explain the different types of corrugation

encountered. Investigations indicate that fastener stiffness, vehicle suspension, rail metallurgy, track geometry, and operating conditions are among factors that affect the development of rail corrugation. These studies, however, do not provide conclusive information on how to alleviate rail corrugation, particularly on transit track.

This digest reports the work undertaken by the Association of American Railroads (AAR) for TCRP Project D-1. In a previous study sponsored by the FTA (FTA-MD-06-0141-93-1), many issues related to rail corrugation on rail-transit track were addressed. Project D- 1 was intended to build on that study and on research into corrugation carried out elsewhere. The aim of Project D-1 was to provide a better understanding of rail corrugation initiation and growth in order to establish the effect of track, vehicle, and operating characteristics on rail corrugation development. A further aim was to develop suitable means for reducing rail corrugation in transit systems.

The program of work carried out by the research team included the following:

- A literature search of corrugation research,
- Comprehensive site visits to transit systems where rail corrugation has occurred,
- Data collection on both the track and the vehicles operating on the track,
- Derivation of parameters characterizing the dynamic behavior of the track and the vehicles,
- Theoretical modeling of possible corrugation mechanisms,

**CONTENTS**

**Introduction, 1**

**Background, 3**

**Findings, 4**

**Conclusions, 8**

**Suggested Further Research, 9**

**APPENDIX A Results of Field Tests, Observations, and Analyses, 9**

**APPENDIX B Comparison of Measured and Calculated Vertical Track Receptances, 17**

**APPENDIX C Wheel Set Test and Modeling Results, 22**

**APPENDIX D Results from Corrugation Initiation Model, 24**

**APPENDIX E Suggested Corrugation Mitigation Measures, 27**

**APPENDIX F Simple Economic Analysis of Potential Corrugation Mitigation Measures, 30**

- Correlation of experimental data with theory, and
- Suggestions for corrugation mitigation on transit track.

It was the contention of the research team that, unless the mechanism of corrugation occurring at the various transit systems was understood, it would not be possible to evaluate which methods of mitigation might be most appropriate. Indeed, the method of mitigation is likely to differ depending on the particular mechanism of corrugation being considered. It was with this in mind that the research team considered it essential to characterize the corrugations, vehicle, and track at each site in order to establish a computer model capable of simulating the principal corrugation mechanisms found. The ability to predict the corrugation mechanism would also permit an understanding of the likely contributing factors and, therefore, the mitigation method most likely to be effective. In addition, the model provides a tool that can be used for assessing the potential benefit of a particular mitigation method. This philosophy determined the test and modeling methodology used to perform the project.

## BACKGROUND

Corrugation and vehicle/track characteristics were obtained from sites at the following transit systems:

- Chicago Transit Authority (CTA),
- Mass Transit Administration of Maryland (MTA),
- Washington Metropolitan Area Transit Authority (WMATA),
- Bay Area Rapid Transit (BART), and
- Sacramento Regional Transit District (RTD).

Rail corrugations were quantified in several ways. An initial visual inspection was performed to determine whether they were formed from longitudinal or lateral wheel/rail forces. Wavelength information was then gathered by using a ruler and a longitudinal rail profilometer.

Mathematical models were developed for the track structure, a flexible wheel set, and a flexible wheel set interacting with the track in order to understand the corrugation mechanisms that occurred at the various sites. Dynamic parameters required for these models, such as inertia, stiffness, and damping, were obtained by measuring wheel set and track receptances at the various sites.

Receptance is the complex ratio of displacement response to an input force and was found by using an instrumented hammer as the means of excitation. The hammer had a hardened steel tip and was fitted with an accelerometer calibrated to provide a measurement of force by hitting a load cell with the hammer. The procedure adopted for the measurement of receptance was to place an accelerometer on the body to be tested and hit the body with the instrumented hammer. The method of hitting was important-it

was essential not to have a rebound hit. The input force and body response for each strike were recorded using a laptop computer loaded with a commercial data collection software package. The transfer function was then reviewed and, if it looked reasonable, it was saved and the procedure repeated so that at least 10 acceptable responses were collected. The transfer functions were then averaged and converted into a receptance.

Wheel set receptances were determined for radial, lateral, and torsional excitation. The radial response was determined by mounting an accelerometer on the wheel tread and hitting the tread with the instrumented hammer at a location opposite the accelerometer location. Lateral response of the wheel set was determined by placing the accelerometer on the face of the rim and striking the rim laterally with the instrumented hammer. The accelerometer was rotated through 90 degrees and mounted on the tread to measure the torsional response of the wheel set. AC-clamp was then attached to the rim to provide a location for excitation by the hammer. In the frequency range 0 to 500 Hz, there was a fundamental torsional mode of the wheels rotating out of phase with each other and a second torsional mode where the wheels move in phase with each other but out of phase with the traction motor drive gear.

Track receptances were found for both vertical and lateral excitation. These were obtained by mounting an accelerometer on the rail and hitting it with the instrumented hammer in the appropriate place. Track receptances were used to find the pad characteristics for direct fixation track and the tie pad, as well as ballast characteristics for concrete and wood tie track.

As far as the vehicle is concerned, any contribution to rail corrugation is likely to come directly from the vehicle unsprung mass. This includes primarily the wheel set, a component from the traction motor, and in some cases, part of the axle bearing boxes and brakes. The unsprung mass becomes increasingly isolated from the rest of the vehicle at frequencies above those of the truck on primary suspension. This is the case for not only vertical motions but also lateral and longitudinal motions of the wheel set. As a result, in the frequency range where corrugations occur, the remainder of the vehicle provides essentially steady forces through the primary suspension. These forces include the vertical load on the wheel set, a lateral force, and yaw moment during curve negotiation, along with any traction or braking torques. Thus, the dynamic modeling of the vehicle's role in rail corrugations was confined to the wheel set in this project.

Previous work on corrugation has produced several theories. Of these, the most promising hypotheses are based on the assumption that corrugation is essentially a periodic wear process. When new rail is laid, the surface roughness is broad band random with no predominant wavelengths present. Any surface roughness can be represented as a combination of sinusoidally varying components with appropriate amplitude and phase relationships. This is the fundamental concept of Fourier Analysis. Fluctuations will occur in

the wheel/rail forces and creepages if a wheel set passes over any one of these constant wavelength components in the rail surface roughness. These fluctuations are influenced by the dynamic characteristics of the wheel set and the track at the resulting frequency. This frequency is defined by the wavelength of the irregularity and the velocity of the wheel set. The fluctuations in wheel/rail force and creepage cause fluctuations in the rate of wear of the rail surface, which will be at the same frequency as the component of surface roughness. If the phase relationship of the fluctuations in wear is such that the peaks of maximum wear correspond to the troughs in the surface irregularity, then the irregularity in the rail surface at that wavelength will grow and corrugations will form at the corresponding wavelength.

A corrugation initiation model was developed using the AAR's NUCARS general rail vehicle dynamics program based on the corrugation formation hypothesis described above. Essential features of the model were as follows:

- A track dynamic model capable of representing either a single- or two-layer track form,
- A wheel set running on the track with appropriate torsional flexibility,
- A detailed wheel/rail creep force model representing non-linear creep saturation effects,
- The ability to represent the wheel set negotiating a curve,
- The ability to apply braking or traction torques to the wheel set,
- The capability for inputting rail surface irregularities, and
- The ability to predict wheel/rail wear fluctuations.

AAR's NUCARS general rail vehicle dynamics program operates in the time domain and provides the capability for modeling any dynamic system consisting of a number of masses with prescribed degrees of freedom coupled by connections with a wide range of available characteristics. It also incorporates a state-of-the-art wheel/rail creep force model that uses a multidimensional look-up table of data generated from Kalker's program "Duvorol." This program is based on Kalker's exact theory and provides the most accurate creep force/creepage data currently available. In addition, the NUCARS program provides output of wheel/ rail wear based on the proportionality of wear to creep force multiplied by creepage. NUCARS can also represent curve negotiation and provides a general input capability for either measured or mathematically generated rail irregularities.

Until recently, NUCARS incorporated only a very simple representation of track flexibility. However, over the last few years, a prototype track model has been developed within NUCARS under a project funded by AAR's research program. This model incorporates a finite length of track with discrete supports that move with the vehicle. NUCARS already provided the capability for representing a torsionally flexible wheel set. In TCRP Project D-1, a model of a

torsionally flexible wheel set running on track was developed using NUCARS and used to predict corrugation.

## FINDINGS

As a result of visits made to the various transit systems (see Appendix A), it was observed that corrugations were associated primarily with curves, particularly on the low rail in curves, and with sites where vehicles were accelerating or braking (i.e., at sites where there would be a significant longitudinal traction or creep force). The general appearance of the corrugations was a rut lying across the rail, the troughs of which were relatively dull, while the peak was distinguished by a fine shiny line across the railhead (Figure 1). It was common to find evidence of longitudinal slip in the corrugation troughs. The only exceptions to this were in locations where a restraining rail was present or where rubber, booted ties (twin block tie mounted in a resilient boot) were used. However, these sites represented a relatively small percentage of the total track length investigated. Consequently, it was apparent to the research team that longitudinal slip and wear are responsible for most corrugations on transit track. The wavelength of the observed corrugations varied from 25 to 100 mm (1 to 4 in.), with a preponderance at around 50 mm (2 in.).

The frequencies associated with the observed corrugations were calculated from the measured wavelengths by estimating the average operating speed of the trains over the corrugated track section. Results showed that most of the longitudinal corrugation frequencies are clustered about the wheel set second torsional mode (Figure 2). Corrugations at one transit system where longer wavelength corrugations were measured showed that the corrugation frequency was similar to the P2 resonance (wheel set bouncing on track stiffness). On another system, the corrugation frequency was similar to the rail "pinned-pinned" bending mode (Figure 3).

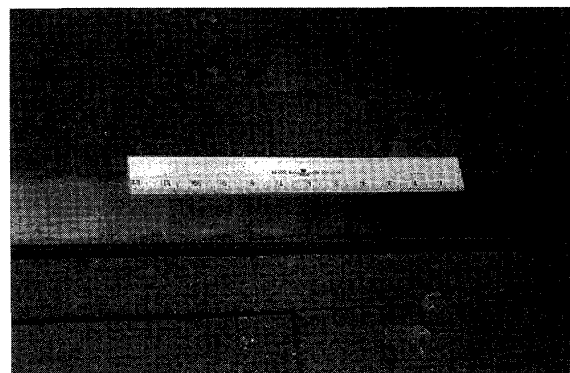


Figure 1. Corrugations at Milwaukee subway on the CTA

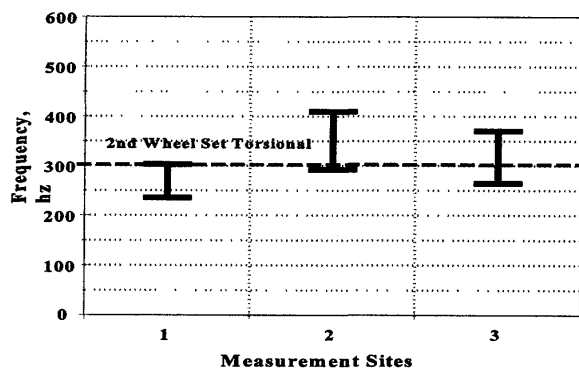


Figure 2. CTA corrugation frequency

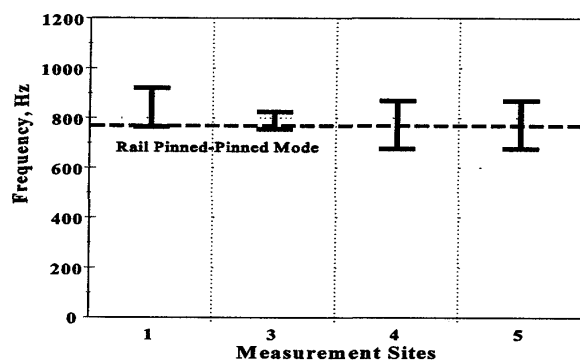


Figure 3 WMATA corrugation frequency

Various forms of track construction were found at the different transit systems. These included direct fixation, ballasted track with wood ties, ballasted track with concrete ties, rubber bootied ties, embedded rail, and elevated steel structures with wood ties. Any of these forms of track can be represented as a rail supported at regular intervals either directly by a rail pad to the ground or on ties which rest on a resilient medium. The medium is usually ballast, except in the case of the rubber bootied tie. Because predominant corrugation mechanism at sites visited appeared to involve longitudinal slip between wheel and rail, a vertical model of the track was developed.

The mathematical model of track traditionally used is that of an infinite Euler beam on a continuous distributed elastic support representing the ballast. In some analyses, damping is included in the support and the mass of the ties has added to that of the rail. Although this simple model has been used extensively, it has deficiencies (e.g., no discrete

periodic support of the rail, no resilient rail pad between rail and tie, and no separate representation of the tie mass).

In this project, NUCARS was used to develop two basic track models, the first was a single-layer model of two flexible rails, 85 m (93 yd) long with regular discrete supports for the rail pads represented as parallel stiffness and viscous dampers to ground. The rail degrees of freedom include flexible degrees of freedom up to the pinned-pinned mode. This model was used for simulating direct fixation track, wood tie track, and embedded track. The second model was a two-layer model with two flexible rails, 22 m (24 yd) long with regular discrete supports through rail pads to rigid ties. The ties interconnect the two rails and are connected to ground through discrete supports representing the ballast. Both the rail pad and ballast are represented as parallel stiffness and viscous dampers. This model was used for simulating concrete tie ballasted track. In each case, track receptances were calculated by applying in-phase swept sine wave vertical forces to both rails at the longitudinal midpoint.

It was necessary to make the direct fixation track model much longer than the concrete tie ballasted track model because experimental track receptance measurements showed that the damping of the direct fixation track was much lighter than that of the ballasted track. Track length was determined by the need to prevent significant reflection of the traveling wave from the end of the model track. (Appendix B contains a complete set of results comparing the measured and calculated vertical track receptances.)

Comparison of measured and calculated responses showed that direct fixation, wood tie ballasted, and embedded track can all be modeled using the single-layer track model. As shown in Figure 4, the receptances exhibit one clearly defined, lightly damped resonant peak in the frequency range of 0 to 500 Hz, which is the frequency range of interest for all but one type of corrugation found during the survey. In addition, any track system also has a rail pinned-pinned mode. Although the frequency of this mode was found to be generally in the range of 370 to 1,100 Hz, it was usually in the range of 600 to 800 Hz.

The lower frequency mode common to all track is associated with the rail bouncing on the vertical track stiffness. The frequency and damping depend primarily on the track support characteristics, but frequency is also influenced by the rail section properties. For the direct fixation track tested, the support stiffness and damping are lower than that for the ballasted track.

The receptance exhibits the same single resonant peak with wood tie ballasted track as is seen with direct fixation track except that the single resonant peak is more heavily damped. The frequency and damping of this peak are controlled primarily by the ballast characteristics. Embedded track also produces a receptance having the single resonant peak characteristic of a single-layer track model, although the stiffness and damping of the support are considerably higher than that of the wood tie track.

In the case of concrete tie ballasted and rubber bootied

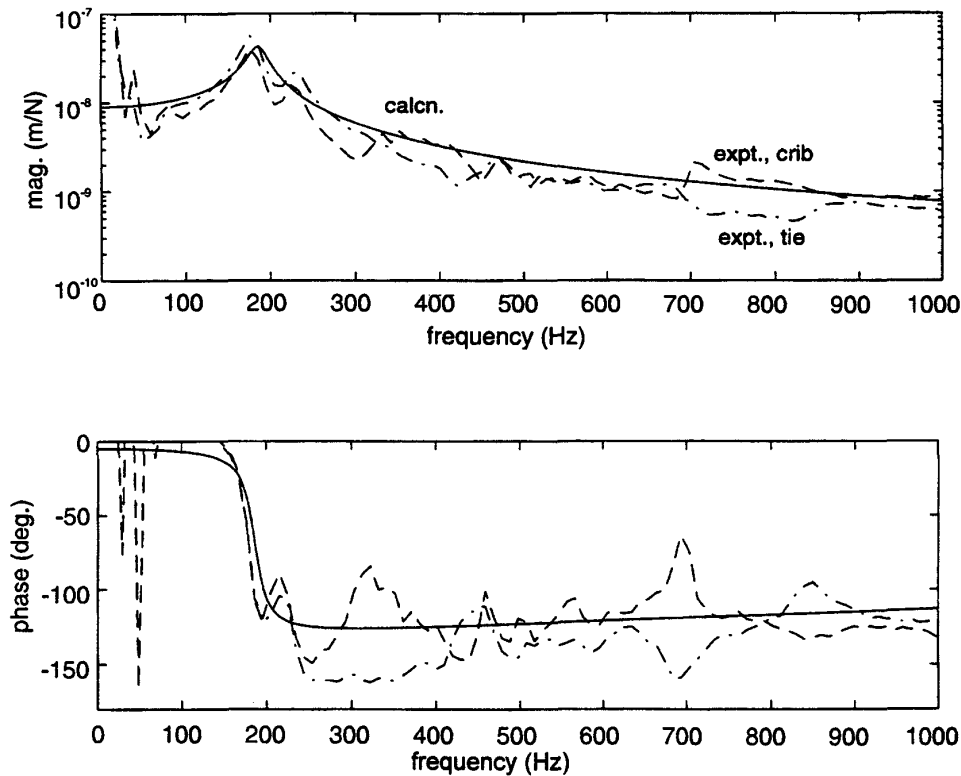


Figure 4. Measured vertical track receptance--BART Site 1.

tie track, it was necessary to use a two-layer track model. With this type of track, two primary peaks were evident in the frequency range below 500 Hz. The first peak is associated with the rail and ties moving in phase on the flexibility of the ballast or tie boot. The second peak is associated with the rail and ties moving in antiphase on the flexibility of the rail pad. There is an intervening anti-resonance in which the rail is essentially stationary. The ties, acting as a vibration absorber, vibrate on the rail pad and ballast or tie boot in parallel.

The booted tie track has characteristics that are quite different from concrete tie ballasted track. The resonant and anti-resonant frequencies of the system are also different. The first resonance was at a lower frequency and the second resonance at a higher frequency. This difference is a result of the boot stiffness being much lower than the concrete tie track ballast stiffness and the concrete tie track having a much softer rail pad.

The vertical track response is particularly important because of the association of several types of corrugation with the so-called P2 or "loaded track" resonance. Typically, the frequency of this mode is less than about 100 Hz. Corrugation wavelengths would be several centimeters long for the typical train speeds found in this study. Only at one site

where corrugations were measured was the wavelength sufficiently long to be associated with the P2 resonance. At this site, there was good correlation between the measured corrugation frequency and the P2 resonance calculated from the measured track and vehicle parameters.

The contribution of the dynamic behavior of the vehicle wheel sets to rail corrugation was investigated in a manner similar to that used for the track structure. The systems, except one, had essentially the same wheel set, traction motor, and final drive arrangement. On these systems, a nosehung traction motor was employed for each axle, with a gear on the end of the armature shaft driving the wheel set directly through a gear mounted on the axle. This gear was typically located about one-third of the distance between the two wheels.

The drive arrangement was markedly different for the light rail vehicles at the Sacramento RTD. Each powered truck included a monomotor with the motor armature. The armature was aligned with the longitudinal track axis and provided the driving torque to both axles through a rightangle drive arrangement. The drive to each axle incorporates a flexible coupling, which essentially isolates the wheel set from the traction motor in the corrugation frequency range. In addition, resilient wheels were used at RTD-the

rim of each wheel was separated from the wheel web by a circle of rubber pads.

Examination of the corrugations on the heavy rail systems indicated that, apart from several sites with a restraining rail and a site with rubber bootied ties, the corrugations were remarkably similar and the surface markings were primarily longitudinal. Further, the corrugation patterns were perpendicular to the longitudinal axis of the rail, indicating that the principal direction of relative wheel/rail motion during corrugation formation was longitudinal. As a result, the wheel set model that was developed included only torsional flexibilities.

The RTD corrugations were also perpendicular to the longitudinal rail axis and showed longitudinal surface markings. However, the frequency of these corrugations—about 600 Hz—was considerably higher than those on the heavy rail systems.

Receptance measurements showed that, for all of the heavy rail systems, there was a fundamental wheel set torsion mode in the range of 50 to 100 Hz and another torsion mode was evident at about 300 to 350 Hz. At 300 Hz, the wheel set is almost certainly decoupled in torsion from the motor armature by the contact flexibility of the gear train. However, the rotational inertia of the final drive gear is rigidly attached to the axle shaft approximately one-third the distance between the wheels. A model of wheel set torsional behavior was developed using NUCARS (Figure 5).

Wheel set drawings of a typical axle shaft and wheel were analyzed to determine shaft stiffness and mass, as well as wheel rotational inertia about the wheel set axis of rotation. In addition, an estimated rotational inertia was used for the final drive gear. The model incorporated the rotational degrees of freedom of the two wheels and the final drive gear connected by the torsional stiffness of the axle shaft. All of the heavy rail systems used basically the same traction system. Their wheel set and primary suspension arrangements were of the following types:

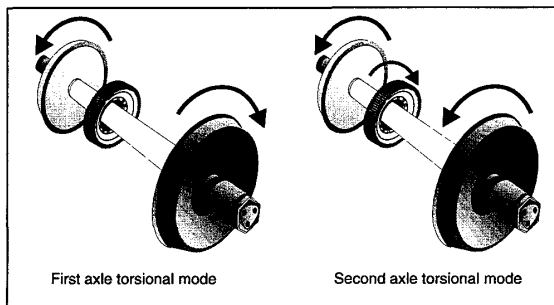


Figure 5. First two powered torsional modes of wheel sets.

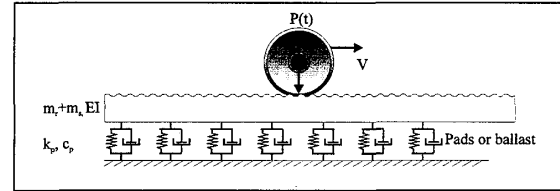


Figure 6 Corrugation formation model

- Inboard axle bearings with a cylindrical rubber bushing for the primary suspension or
- Outboard axle bearings with a chevron primary suspension.

The modal characteristics of wheels are dominated by the rim mass and stiffness characteristics with the wheel plate acting essentially as a diaphragm that restrains the rim radially. As a result, the wheel set modal characteristics for all the heavy rail vehicles were very similar.

The light rail system at the Sacramento RTD had a monomotor arrangement driving both axles of a powered truck through flexible couplings. The primary suspension used outboard bearings and chevron springs, and the wheels incorporated a resiliently mounted rim. This arrangement significantly altered the wheel set modal characteristics compared with the heavy rail vehicles. (Appendix C contains the wheel set test and modeling results.)

The NUCARS model of a single wheel set running on a model of the track was used to simulate the corrugation initiation mechanism (Figure 6). In this model, it has been assumed that steady longitudinal forces are present on each wheel because of either traction or braking demands or curve negotiation. The wheel set track model demonstrated the presence of a corrugation initiation mechanism at around 100 Hz. Initial randomly distributed irregularities on the surface of the rail would be expected to cause a corrugation to grow at a wavelength corresponding to about 100 Hz for the appropriate vehicle speed (Figure 7). This occurs because the fluctuating rail wear resulting from the wheel running over the surface irregularities has a maximum at this frequency and the positions of maximum wear coincide with the troughs in the surface irregularity. The growth rate of this type of corrugation would almost certainly be accelerated if the fundamental wheel set torsion mode frequency was close to the P2 frequency. (Appendix D contains the results from the corrugation initiation model.)

A second corrugation initiation mechanism involving a wheel set torsional mode was also predicted by the model. The mode in question is the second torsional mode of a wheel set with a final drive gear. This mode occurred in the frequency range of about 300 to 350 Hz for the heavy rail properties. In this case, the model indicates that corrugations would form on one rail because of the surface irregularities in the other rail (Figure 8). Observations of corruga-

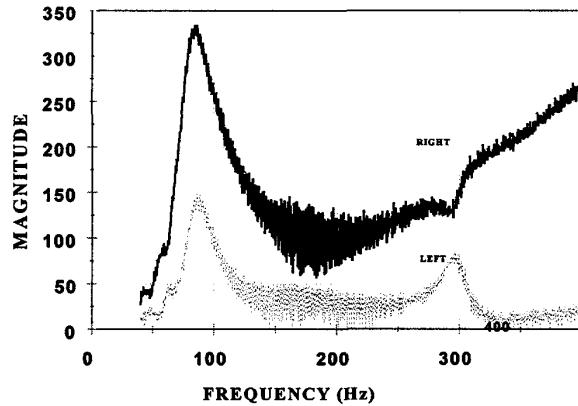


Figure 7. Magnitude of wheel wear/irregularity transfer function--single-layer track

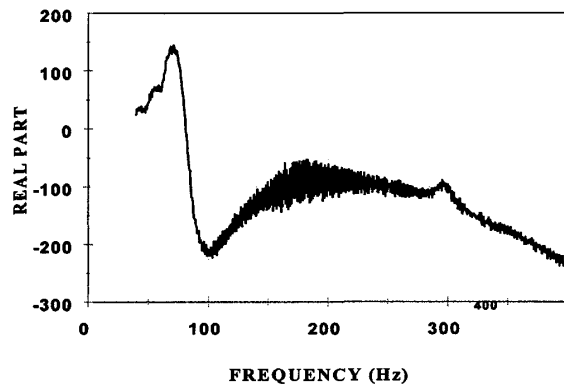


Figure 8. Real part of right wheel wear/track irregularity transfer function--single-layer track

tions tend to support this possibility in that corrugations were seen on the rail opposite to rail joints.

## CONCLUSIONS

A combination of field observations, measurements, and computer modeling has been used to characterize the types of rail corrugation occurring on U. S. transit system track. On the Sacramento RTD, the only light rail system investigated, a type of corrugation was found that was different from anything seen at the heavy rail systems. This type of corrugation occurred at all RTD sites and had a relatively short wavelength with the appearance of the so-called "roaring rail" corrugations. However, several different corrugation mechanisms were found at the heavy rail sites; these could be categorized as follows:

- Type 1: P2 resonance (BART only),
- Type 2: Second wheel set torsional mode (all heavy rail properties),
- Type 3: Lateral associated with restraining rail (BART only),
- Type 4: Lateral associated with booted tie track (MTA only), and
- Type 5: Primarily rail pinned-pinned mode related (WMATA only).

Type 3 corrugations were found only at BART. These corrugations were found at curve locations equipped with restraining rails. Type 4 corrugations were found only at MTA on locations equipped with rubber booted ties. Type 5 corrugations, which seem to be associated with the rail pinned-pinned bending frequency, were only found at WMATA. The locations where Type 3, 4, and 5 corrugations occurred represent a relatively small percentage of the total transit track length surveyed.

Both Type 1 and Type 2 corrugations are associated with longitudinal wheel/rail slip. Type 1 corrugations, related to the P2 resonance, were found only on direct fixation track at BART. Predictions with the model showed that this type of corrugation is only likely to occur where the track support stiffness is high and the track support damping is low. BART had the highest direct fixation track support stiffness and the lowest track support damping of any of the heavy rail properties visited. On the basis of these observations, it is concluded that Type 1 corrugation may be reduced by decreasing the vertical stiffness of the rail pad or increasing its damping.

Type 2 corrugations, which appear to be associated with the second wheel set torsional mode, were present at all of the heavy rail properties. As a result, it was concluded that efforts to develop corrugation mitigation methods should concentrate on addressing Type 2 corrugations.

The modeling of potential mitigation methods showed that changes to the track support characteristics would have no effect on the development of Type 2 corrugations. This result is supported by the site observations indicating Type 2 corrugations were present on all the heavy rail systems surveyed on almost all types of track structure, including direct fixation, concrete or wood tie on ballast, wood blocks set in concrete, overhead viaducts, elastic fastenings, or spikes. The formation of these corrugations depends on the presence of longitudinal wheel/rail forces. These are generated either by traction or braking demands, by longitudinal forces resulting from curve negotiation, or a combination of the two.

The application of gage face lubrication in curves or modifications to the truck primary suspension would reduce the longitudinal forces produced during curve negotiation; however, longitudinal forces generated by traction and braking demands would still be present. Acceleration and braking occurs frequently on most transit systems. Thus, improved truck curving performance on its own is not a means



of addressing this type of corrugation. Reducing longitudinal forces resulting from traction and braking would involve decreasing the current maximum acceleration and stopping rates. This would almost certainly be unacceptable to transit agencies.

This leaves the following possibilities for alleviating the development of Type 2 corrugations:

- Use of more wear-resistant rail materials,
- Controlled railhead lubrication, and
- Changing the wheel set and drive arrangement torsional characteristics.

Although more wear-resistant rail materials would reduce the rate of corrugation development, this would not influence the fundamental corrugation mechanism. Controlled railhead lubrication should reduce the corrugation development rate directly by reducing the wheel/rail friction coefficient. This could also influence the response of the wheel set in its second torsional mode. However, railhead lubrication would have to be very carefully controlled in order not to cause wheel spin under traction or wheel slide under braking.

The most direct means of addressing this type of corrugation is through changes to the torsional dynamic characteristics of the wheel set and traction motor arrangement in order to influence the properties of the second torsional mode. This could involve changing the frequency or providing additional damping. Both could reduce the corrugation development rate and completely change the initiation mechanism.

Various methods of changing the torsional characteristics of the wheel set and drive arrangement are possible. These include using resilient wheels, resiliently mounted final drive gear, and torsional vibration absorbers.

Resilient wheels have a damping layer inserted between the plate of the wheel and the rim. This has the effect of reducing the amplitude of vibration between the wheel and its rim. There are several ways in which a flexible mounting can be arranged between the final drive of the motor and the axle. The use of such a mounting will change the torsional vibration characteristics of the axle.

Several companies manufacture vibration absorbers for railway wheels. These act in the lateral direction on the wheel rim or wheel plate and are primarily used for noise suppression.

As far as the practical control of corrugation is concerned, it follows that, even if it were not possible to eliminate all types of corrugations, a more modest but nonetheless useful goal would be to eliminate the more severe types of corrugation. Appendix E suggests corrugation mitigation measures pertaining to the track and to the vehicles.

Although a full assessment of the economic viability of the proposed mitigation methods was not possible within the time frame and resources for this project, a simple economic analysis has been carried out in Appendix F. Appendix

F provides a comparison of relative annual costs for the various corrugation mitigation measures as they relate to grinding as the base case measure for corrugation control.

The information contained in appendixes E and F provide guidelines to transit systems about how to deal with the various types of corrugation and the costs involved.

## SUGGESTED FURTHER RESEARCH

AAR suggests that the Type 2 corrugation, which appears to be the most predominant type on U.S. transit track, be investigated further. This type of corrugation appears to be associated with the second torsional mode of a powered wheel set and is influenced by longitudinal wheel/rail forces resulting from traction, braking, or curving.

## APPENDIX A

### RESULTS OF FIELD TESTS, OBSERVATIONS, AND ANALYSES

#### TEST SITES AND GENERAL OBSERVATIONS

The general comments and observations made in this appendix derive largely from conversations with the transit system personnel who assisted the AAR measuring team and selected the measuring sites. Quantitative measurements have not been made to check statements regarding matters such as the prevalence of corrugation on different types of track form.

#### CHICAGO TRANSIT AUTHORITY (CTA)

Three sites covering a range of track forms were selected for measurement at CTA. The first site, in a tunnel, was constructed in the 1950s; the second, on an elevated, steel structure typical of many traditional U.S. transit systems, was constructed in the early 1900s; the third, on track with wood ties in ballast, was constructed in 1983. Details of all sites are given in Table A-1.

Corrugation is an endemic problem on the track at CTA and exists, to some extent, on all lines. Although the transit authority owns a shuffle-block rail grinder, use of the grinder does not fully address the corrugation problem. Corrugation is believed to have become much more severe in the 1950s following the introduction of lightweight vehicles with high traction and braking rates; a figure of 4.5 km/h/s was mentioned for the latter. Vehicles on CTA have electromagnetic track brakes. Although these are intended for emergency use only, there are signs of their frequent use on the approach to stations; the rail appears "ground" by the track brakes. CTA

**TABLE A-1 CTA track site and corrugation characteristics**

<b>CHICAGO (CTA)</b>									
<b>Site</b>	<b>Name</b>	<b>MP,CM, etc.</b>	<b>Curve, super</b>	<b>Rail</b>	<b>Support</b>	<b>Spacing (meters)</b>	<b>Corrugation Wavelength (millimeters)</b>	<b>Corrugation Direction</b>	<b>rail pinned-pinned frequency(Hz)</b>
1	Milwaukee Subway,Blue line	-	no	100RE	wood blocks, spikes	0.46	66	Longitudinal	650
2	California Station	-	no	90AS	wood ties, spikes	0.46	38	Longitudinal	620
3	Irving Park	-	gentle	100RE	wood ties, ballast, spikes, plates	0.61	42	Longitudinal	370

was thought to be the only North American transit system using such brakes.

As a result of the stations at CTA being quite close together, vehicles are almost always either accelerating or braking, both of which give rise to high demands on longitudinal traction at the wheel/rail contact. In view of the research team's findings regarding the most likely corrugation mechanism on this system, this is probably a significant reason for there being such widespread and severe corrugation at CTA. Because of the severe curves on the elevated structures, which follow the roads below, vehicles are relatively short and, consequently, have a relatively large number of axles.

The original track form at CTA comprises 90AS rail spiked to full length or stub wood ties with an 0.46-m spacing. The rail now used is 100RE section; where possible, this is laid on supports at 0.61-m spacing.

The first site on CTA was on tangent track in a subway about midway between stations. Here the rail is spiked to cedar stub ties which are cemented into the tunnel invert.

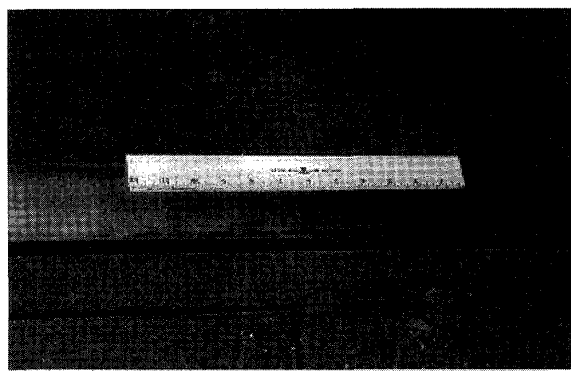


Figure A-1. CTA Site 1

The corrugation appears uniformly periodic and is apparent as a bright band (the corrugation peak) running right across the rail, with duller material between the crests (Figure A-1). This is typical of the type of corrugation referred to as rutting (1). The average wavelength was 66 mm.

The second site was on a steel elevated structure characteristic of older U.S. transit systems. Here, full-length wood ties rest on the steel structure; every third tie is secured to the steel structure with a J-clamp. The site was on the run from California station; accordingly, vehicles would be accelerating with high traction. Corrugations at this site appeared similar to those in the tunnel (Figure A-2), although the wavelength was rather lower (38 mm). Heavy longitudinal slip marks were apparent in the corrugation troughs.

The third site at CTA is on track with base plates and wood ties laid in ballast. This track, which has elastomeric tie-saver pads between the base plates and the wood ties, is on a very gentle curve on the run out of Irving Park station. The corrugation here is of similar wavelength (42 mm) to that at Site 2 and also of similar appearance. The power spectral density (PSD) of the corrugation wavelength data is shown in Figure A-3 and the corrugations themselves are pictured in Figure A-4.

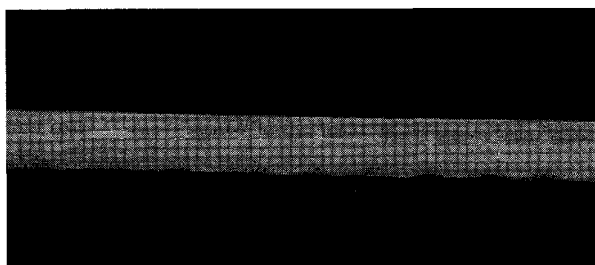


Figure A-2. CTA Site 2

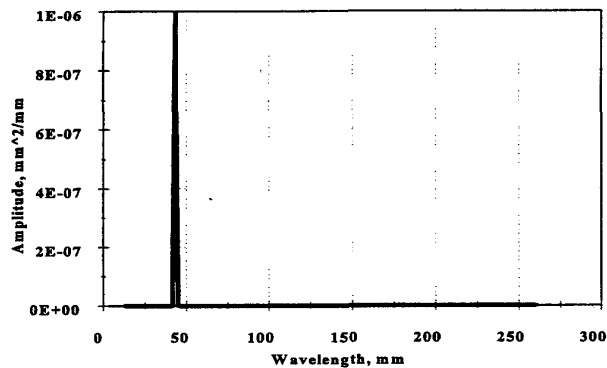


Figure A-3. PSD of corrugations measured on CTA Site 3.

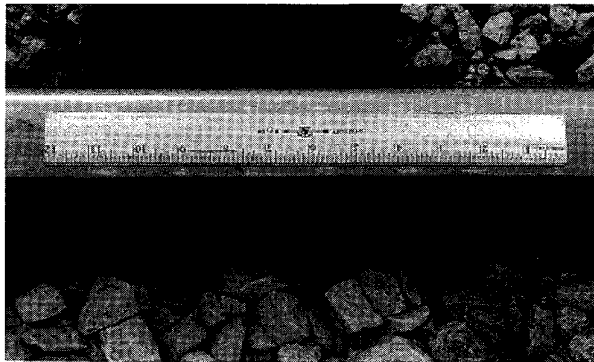


Figure A-4. CTA Site 3.

## MASS TRANSIT ADMINISTRATION OF MARYLAND (MTA)

The MTA system consists of 48 km of track extending over 24 km of route. There is a wide variety of track forms. Corrugation exists on all types of track form. Despite the literature discussing corrugation on the rubber bootied-tie track form on this transit system, the present track maintenance personnel did not think corrugation was more or less prevalent on any particular track form. Corrugation was, however, associated with braking and downhill sites more than with accelerating and uphill sites. Measurements were made at six MTA sites, details of which are given in Table A-2.

Lubrication at MTA is primarily by solid lubricant sticks on the vehicles. This is supplemented by manual greasing of the high rail only in severe curves. Manual greasing is undertaken weekly by spreading about a 0.3-m-long bead of grease every 30.5 m; more frequent or more generous greasing can cause problems with wheel slip. There is one in-track lubricator, near some switches at Johns Hopkins Station.

The track at MTA is almost entirely of 115RE rail with a 0.76-m tie or fastening spacing. Sites 1 and 2 are on adjacent concrete viaducts with different track forms on the same 1,550-m radius. At the first site, there are Hixon direct fixation fasteners at a spacing of 0.91 m; at the second site, there are monoblock concrete ties in ballast with a spacing of 0.76 m. The corrugation wavelengths at the two sites were very different—70 mm at the first site and 28 mm at the second. Corrugation ran continuously on the high rail through the first site, and from about 10 m from the end of the bridge on the low rail (Figure A-5). The corrugation differs in appearance from that of the corrugation on CTA, for example, and is apparent more from discontinuities in the martensitic white phase on the railhead, rather than from there being thin shiny bands lying fully across the railhead. Nevertheless, such marks as did exist on the railhead were primarily longitudinal. Corrugation at Site 2 was less pronounced.

The third measuring site at MTA is on twin block concrete ties mounted in resilient boots. This track form on the MTA has been associated by Ahlbeck and Daniels (2) with a particular type of corrugation arising in part because of there being lightly damped resonances of the concrete blocks and the resilient boots, giving rise to the high amplitude of response to lateral excitation at the railhead. The corrugation noted at Site 3 had a rather scalloped appearance (Figure A-6) which differs significantly from that of the corrugation on CTA. However, this appearance is typical of corrugation on bootied ties (2, 3).

The fourth site at MTA is only a few chains from the third site on the same track, but the corrugations here were of significantly different appearance, with much more evidence of longitudinal slip in the corrugation troughs (Figure A-7). The track here is, however, laid on direct fixation fasteners. This is consistent with the type of corrugation at Site 3 being associated with the bootied-tie track form. Corrugation wavelengths differed slightly at the two sites—71 mm at Site 3 and 53 mm at Site 4. The corrugation at Site 4 is strikingly similar in appearance to that seen at CTA (Figures A-1 through A-4).

Corrugation at Sites 5 and 6 at MTA was similar in appearance to that at Site 4. At Site 6, which was on the approach to Johns Hopkins Station, the average wavelength was 75 mm, but decreased closer to the station. This is consistent with the corrugation being formed by a constant frequency phenomenon, with a wavelength which accordingly decreases as the vehicle speed decreases.

TABLE A-2 MTA track site and corrugation characteristics

BALTIMORE (MTA)									
Site	Name	MP, CM, etc.	Curve, super	Rail	Support	Spacing (meters)	Corrugation Wavelength (millimeters)	Corrugation Direction	Rail Pinned-Pinned Frequency
1	Old Court-Owings Mills	CM572, Track 2	700 m	115RE	Hixson	0.91m	70 mm	Longitudinal	500 Hz
2	Old Court-Owings Mills	CM580, Track 2	700 m	115RE	concrete ties, ballast	0.76 m	28 mm	Longitudinal	710 Hz
3	Tunnel, Track 2	CM202	365 m 100 mm	115RE	twin block, resilient boot	0.76 m	71 mm	Lateral	710 Hz
4	Tunnel, Track 2	CM206.5	365m 100mm	115RE	Hixson	0.91 m	53 mm	Longitudinal	500 Hz
5	Tunnel, Track 2	CM212	365m 100mm	115RE	Hixson	0.91 m	64 mm	*	500 Hz
6	Johns Hopkins Station Approach	*	*	115RE	Concrete ties, 1" thick pads	0.6 m	57 mm	Longitudinal	*

\*No data was recorded.

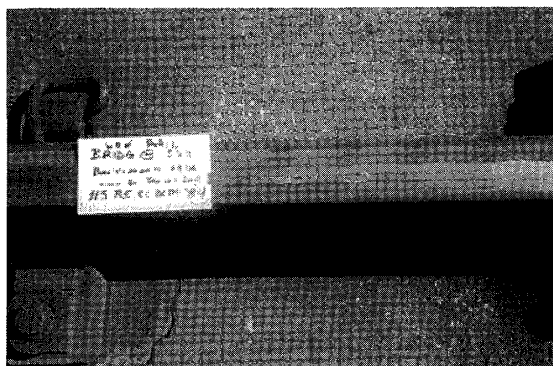


Figure A-5. Corrugations found at MTA Site 1.

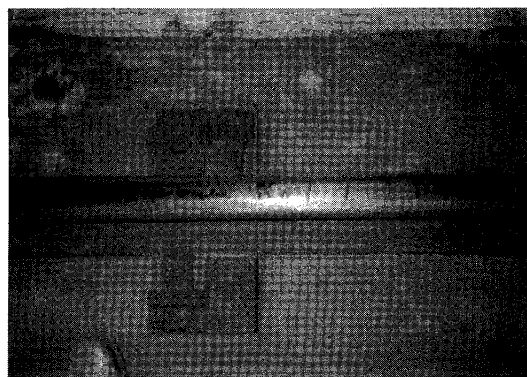


Figure A-7. Corrugations found at MTA Site 4.

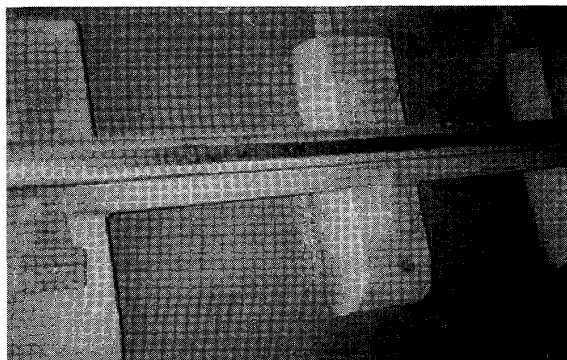


Figure A-6 Corrugation found at MTA Site 3.

#### WASHINGTON METROPOLITAN AREA TRANSIT AUTHORITY (WMATA)

The WMATA system comprises 144 km of route and 300 km of track. Corrugation was associated only with curves of less than a 460-m radius, regardless of the track form, and was thought to be particularly severe in curves of less than a 230-m radius.

There are track forms with direct fixation fastenings (both Hixson and WMATA's own design of plates) and with wood ties and cut spikes on ballast. Corrugation was associated with both types of track form, but was thought to be more severe on direct fixation track. Measurements were taken at seven sites on a variety of track forms, as shown in Table A-3.

TABLE A-3 WMATA track site and corrugation characteristics

WASHINGTON (WMATA)									
Site	Name	MP, CM, etc.	Curve	Rail	Support	Spacing	Corrugation wavelength (millimeters)	Corrugation Direction	Rail Pinned-Pinned Frequency
1	Inbound Blue Line	CM658	650 m 100 mm	115RE	Hixson	0.76 m	32 mm	Longitudinal	710 Hz
2	Inbound Blue Line	near site 1	650 m 100 mm	115RE	wood ties, ballast, spikes, plates	0.70 m	*	*	850 Hz
3	Shaw Howard to U-Street, Tunnel	EL 6200	400 m	115RE	WMATA plates	0.76 m	32 mm	Longitudinal	710 Hz
4	Smithsonian to L'Enfant Plaza Tunnel	D2 5900		115RE	Hixson plates	0.76 m	23 mm	Longitudinal	710 Hz
5	Capitol South to Eastern Market Tunnel	CM127 +70	291 m	115RE	WMATA plates	0.76 m	23 mm	Longitudinal	710 Hz
6	Capitol South to Eastern Market Tunnel	CM127 +50	291 m	115RE	WMATA plates	0.76 m	48 mm	Longitudinal	710 Hz
7	Capitol South to Eastern Market Tunnel	CM124 +70	291 m	115RE	WMATA plates	0.76 m	48 mm	Longitudinal	710 Hz

\*No data was recorded.

Although WMATA initially ran with cylindrical wheels, the wheels are now profiled. Lubrication is done only in the yards.

Seven sites were examined at WMATA on a variety of different track structures. On this system, corrugation was typically at a relatively short wavelength and was more prominent over the fastening or tie than in the crib between ties or fastenings. The corrugation appeared primarily as quasi-periodic patches of "white phase"; the thin, bright, martensitic layer which is common on the running surface of rails (Figure A-8). The fine striae of white phase are aligned essentially along the axis of the rail, which is indicative of their being formed by longitudinal slip. Although these characteristics are typical of the type of corrugation which is seen on high-speed, tangent, or gently curved track, carrying primarily traffic with light axle loads (3), the corrugation sites at WMATA were on fairly severely curved track.

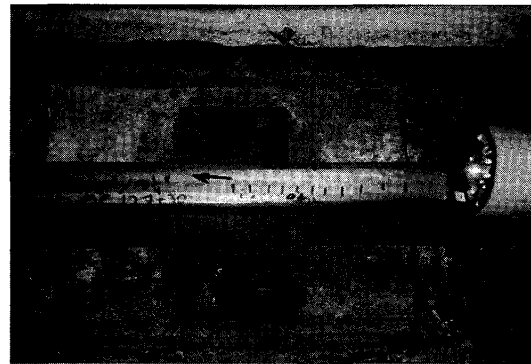


Figure A-8. Corrugations found at WMATA.

TABLE A-4 BART track site and corrugation characteristics

BAY AREA (BART)									
Site	Name	MP,CM, etc.	Curve, super	Rail	Support	Spacing (meters)	Corrugation Wavelength (millimeters)	Corrugation Direction	Rail Pinned-Pinned Frequency
1	Tunnel, M2 Track	M2 0.32	190 m	119RE	Landis	0.76 m	114	Longitudinal	710 Hz
2	Tunnel, MX track	MX 0.32	180 m	119RE	Hixson	0.76 m	34	Longitudinal	710 Hz
3	Orinda station	MP 8.35	no	119RE	concrete ties, ballast	0.76 m	74	Longitudinal	710 Hz
4	Tunnel, M1	M1 0.21	260 m, 45 mm	119RE	DF	0.76 m	*	*	710 Hz
5	Tunnel, Inbound; Webster & 10th	M1 0.27	183 m, 114 mm	119RE	DF	0.76 m	75-High Rail 21-Low Rail 86-Low Rail	Longitudinal Lateral Longitudinal	710 Hz

\*No data was recorded.

#### BAY AREA RAPID TRANSIT, SAN FRANCISCO (BART)

The BART system was built in the 1960s and has various track structures and track forms; about one-third of the system is in tunnels with direct fixation fasteners (both Landis and Hixson) on a concrete base, one-third with wood ties on ballast, and one-third with direct fixation fasteners on concrete viaducts. Corrugation was not associated with curves or with acceleration and braking sites. Measurement was undertaken at five sites, the details are given in Table A-4.

Curves at BART of less than a 183-m radius were constructed with a restraining rail, whereas less severe curves had no restraining rail. Although corrugation occurs on curves of both more wave and less than a 970-m radius, it was found that the restraining rail has an extremely significant effect on the type of corrugation which occurs. This is discussed in the corrugation measurement section.

On BART, 119 RE rail is used throughout the system, and there is a uniform 0.76 m fastener or tie spacing, regardless of the type of rail support. There were five test sites on this system-four of which (Sites 1, 2, 4, and 5) were in curves.

One of the most interesting observations made about BART was that the appearance and wavelength of the corrugation were significantly different on those sites where there was no restraining rail because the curve radius was slightly greater than 183 m. For example, at Site 1 (190-m-radius curve) the corrugation was a relatively long wavelength (108 mm) and the predominant noise of a passing train was of a relatively low frequency rumble. These corrugations are



Figure A-9 Corrugations found at BART Site 1.

shown in Figure A-9. On the other hand, Sites 2 and 5 were in curves of about 180-m radius, and the noise of a passing train was more a high-pitched, extremely loud howling, which would be consistent with excitation of a wheel set lateral resonance. Corrugation on the latter sites was of relatively short wavelength.

On the rails (at Site 5 in particular) there was considerable evidence of high tangential tractions, with severe shearing of the surface material in the running band. On the high rail, shearing was primarily in the direction of traffic, whereas on the low rail, shearing was in the opposite direction to traffic. This is consistent with the longitudinal tractive forces which the trailing wheel set of a truck exerts on the rails

TABLE A-5 RTD track site and corrugation characteristics

SACRAMENTO (RTD)									
Site	Name	MP,CM, etc.	Curve, super	Rail	Support	Spacing (meters)	Corrugation Wavelength (millimeters)	Corrugation Direction	Rail Pinned- Pinned Frequency
1	N Line	MP7.25	610 m 50 mm grade	115RE	Wood ties, ballast, cut spikes, tie anchors	0.61 m	25	Longitudinal	1100 Hz
2	N Line Inbound	MP7.01	no	115RE	Wood ties, ballast, cut spikes, tie anchors	0.61 m	28	Longitudinal	1100 Hz
3	K Street Mall, N Line Inbound	MP0.45	no	115RE	embedded	n/a	23	Longitudinal	n/a
4	F line, West End Brighton Bridge	MP4.85	150 m 12.5 mm	115RE	DF	0.76 m irregular	25	Longitudinal	710 Hz
5	Car Shop Yard, Car on Track	*	no	115RE	Wood ties, ballast, cut spikes	0.61 m	*	*	1100 Hz

\*No data was recorded.

#### SACRAMENTO REGIONAL TRANSIT DISTRICT (RTD)

The RTD system is essentially a modern streetcar or light rail system. The system comprises 30 km of route and 58 km of track. Lubrication is primarily by solid-stick lubricators acting on the wheel flanges; this is supplemented by manual greasing, at weekly intervals, of the high rail in tight curves.

There is a variety of track forms and structures on the RTD system. The system is the only one of the five examined where there was rail embedded in the roadway. Corrugation was not associated with any particular track form or structure. Measurements were made on track in five different locations, details of which are given in Table A-5.

RTD was unique among the five systems in that the traction system comprises a monomotor on each truck driving the wheels through a resiliently mounted gear. The vehicles also have resilient wheels (i.e., the wheel rims are mounted resiliently, essentially in order to reduce noise).

There were four RTD sites at which corrugations were measured, and a further site in the yard of the car shop where measurements were taken only of dynamic characteristics of the track. At all sites, the corrugation wavelength was in the range of 20 to 30 mm. There was considerable white phase in the running band on the rail head, with the white phase being in distinct longitudinal streaks. The severity of these longitudinal marks may arise in part from the severe ma-

chining marks which were observed on the wheel treads. The corrugation was apparent essentially as discontinuities in the white phase, so that the corrugation peaks appeared as discrete patches of white phase.

#### CORRELATION OF OBSERVATION AND MEASUREMENTS

As indicated in Tables A- 1 through A-5, corrugations at the transit agencies primarily developed from a longitudinal process. Where a significant lateral component was observed a significant difference in track structure was found. In BART, the scalloped corrugations appeared only in curves with restraining rails. This makes sense, because the restraining rail would increase the lateral creepages on all axles during curving. At MTA, this lateral nature was only found in the track constructed using booted ties.

Figures A-10 through A-14 show the corrugation frequency range (determined from operating speed range over the site) by site and overlays some of the critical system frequencies which could be related to the corrugations.

These plots were constructed with an assumed speed range of +/- 5 km/h of the speed provided by the transit agency. These plots show, in general, that most of the longitudinal corrugation frequency ranges are clustered about the second wheel set torsional mode. The main exception to this is WMATA where some sights are grouped there, but most

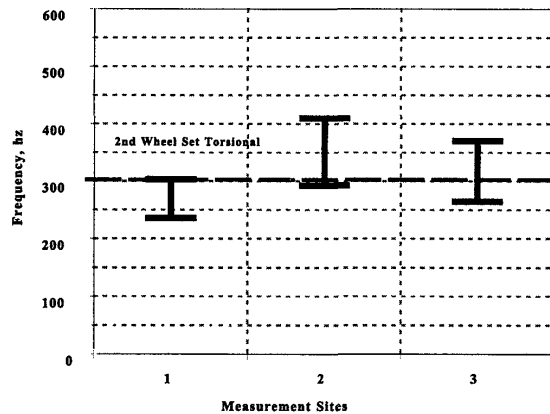


Figure A-10 CTA corrugation frequency

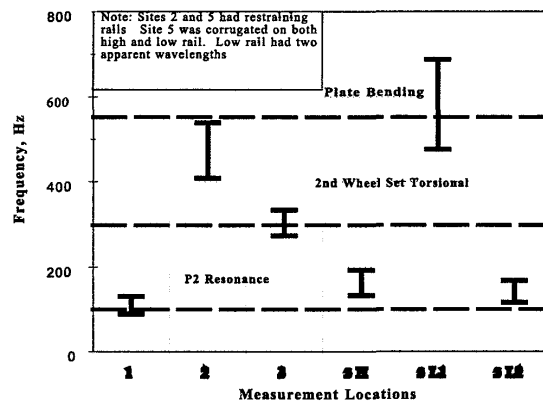


Figure A-13 BART corrugation frequency

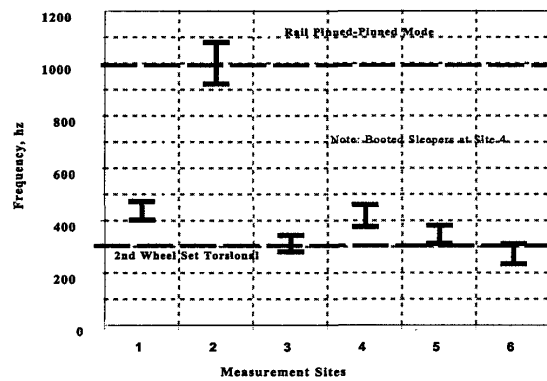


Figure A-11 MTA corrugation frequency

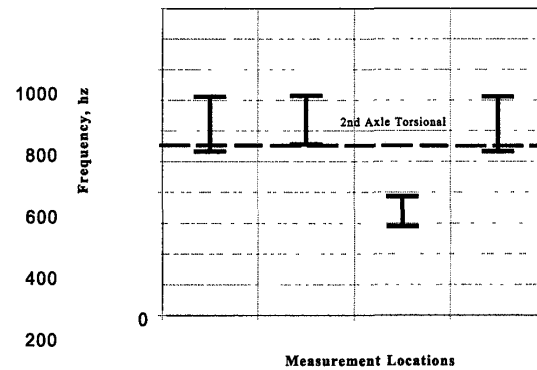


Figure A-14 RTD corrugation frequency

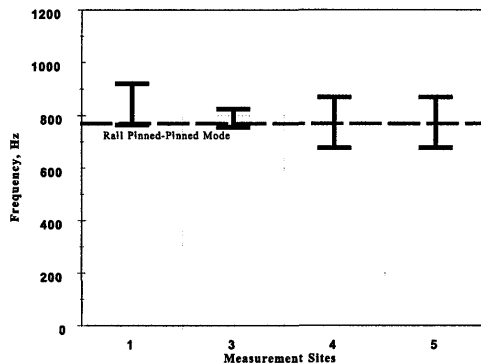


Figure A-12 WMATA corrugation frequency

of the measured sites appear to be related to the pinned-pinned frequency of the rail.

These results are critical to the remainder of the study. They show that, even though a wide range of wavelengths were measured, only a few frequencies are actually of interest. More importantly, knowing the excitation mode allows for models to be assembled which can verify or disprove this hypothesis. Consequently, the modeling can also be focused on the most pervasive corrugations present (i.e., those related to the second axle torsional mode).

## REFERENCES

1. Grassie, S.L. and Kalousek, J. "Rail Corrugation: Characteristics, Causes and Treatments." Proc. Inst. Mech. Engrs., 207 d, pp 57 -68, 1993.



2. Ahlbeck, D.R and Daniels, L.E. "Investigation of Rail Corrugations on the Baltimore Metro." *Wear* 144, pp. 197-210, 1991.
3. Daniels, L.D. "Rail Transit Corrugations, Final Report" FTA-MD-06-0141-93-1, Federal Transit Administration, U.S. Department of Transportation, Washington, DC, 1993.

## APPENDIX B

### COMPARISON OF MEASURED AND CALCULATED VERTICAL TRACK RECEPTANCES

The measured track receptances were determined using an impulsive excitation with an instrumented hammer. Track receptances were calculated by applying in-phase swept sinewave vertical forces applied to both rails at the longitudinal midpoint. Forcing point receptances were then calculated using the same technique as for the hammer blows. This process used Fourier Transform techniques. Track sup-

port parameters were found by correlation of the measured track receptance.

Appropriate section properties for the rail at each site were obtained from the American Railway Engineering Association's manual. These properties included mass per unit length and second moment of area for vertical bending about the neutral axis. Railpad, tie, and ballast characteristics were then varied to provide the best possible match between measured and calculated vertical receptances.

### DIRECT FIXATION TRACK

Dynamic characteristics of direct fixation track using a resilient fastening system were measured at all of the agencies visited except CTA. The track construction in tunnels encountered at CTA consisted of wooden blocks set in concrete to which the rails were spiked. Good correlation was obtained between calculated and measured receptances for all examples of direct fixation track. A typical example from BART is shown in Figure B-1. The support stiffness and damping thus found for different examples of direct fixation track are shown in Table B-1

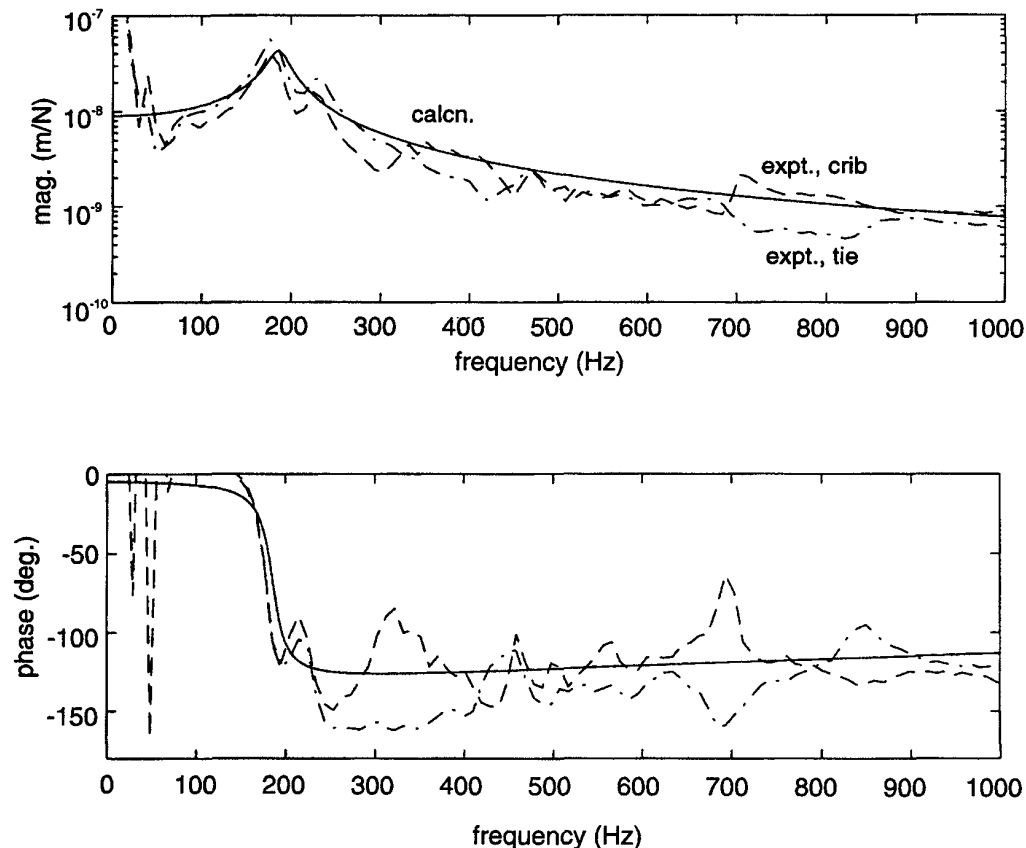


Figure B-1. Measured vertical receptance-BART Site 1

TABLE B-1 Direct fixation track characteristics

Property	Site	Pad Stiffness (MN/m)	Pad Damping (kN.sec/m)	Pad Spacing (m)
MTA	4	18	8.7	0.91
WMATA	1	30	7.4	0.76
WMATA	3	30	7.4	0.76
WMATA	4	30	7.4	0.76
BART	1	61	6.4	0.76
RTD	4	19	3.5	0.76

### WOOD TIE BALLASTED TRACK

Examples of wood tie track were measured at CTA, WMATA, and RTD. When performing receptance measurements on track, it is preferable to have the track loaded with a vehicle. This is particularly the case with ballasted track in order to mitigate the effect of voids between the ties and ballast. Unfortunately, it was not possible to organize the availability of a vehicle for this purpose on revenue service

TABLE B-2 Wood tie ballasted track characteristics

Property	Site	Ballast Stiffness (per rail seat) (MN/m)	Ballast Damping (per rail seat) (kN.sec/m)	Tie Spacing (m)
RTD	5	73	26	0.61

track, but at RTD, receptance tests were performed with a vehicle on wood tie ballasted track in the yard of the vehicle maintenance facility. Figure B-2 shows the correlation between the track model and the experiment for this site and Table B-2 provides the characteristics that were extracted from the model.

At RTD, measurements were also made of the receptance of unloaded ballasted track with wood ties. The receptance, which is shown in Figure B-3, is simply that of a beam in free space. Support characteristics cannot be found from such data. All measurements made elsewhere on wood tie ballasted track were similar to this.

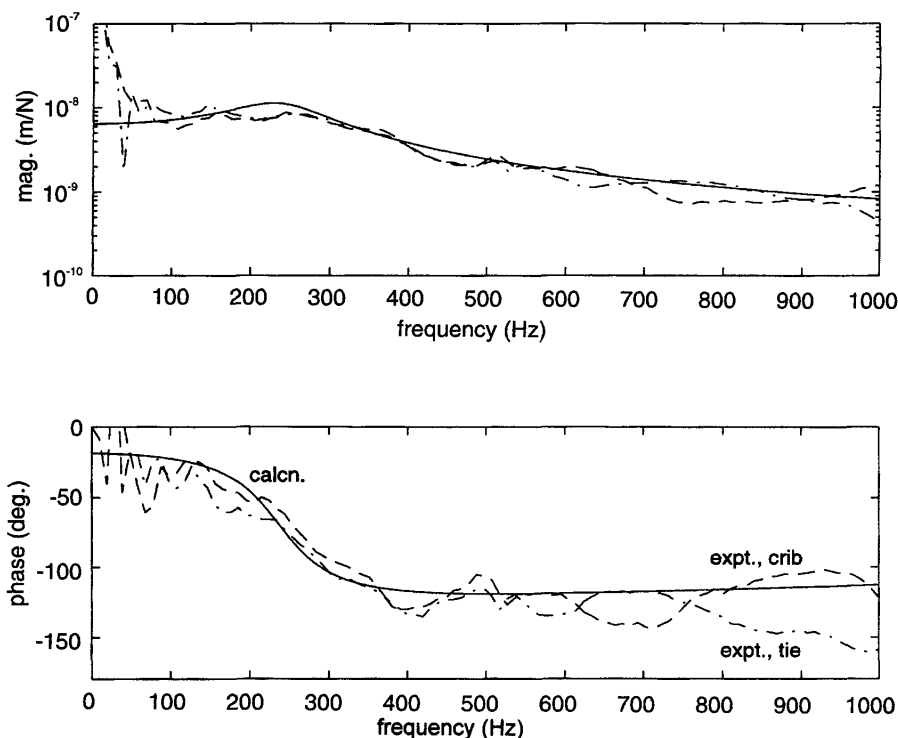


Figure B-2 Measured vertical track receptance -RTD Site 5 (Wood ties in ballast, loaded)

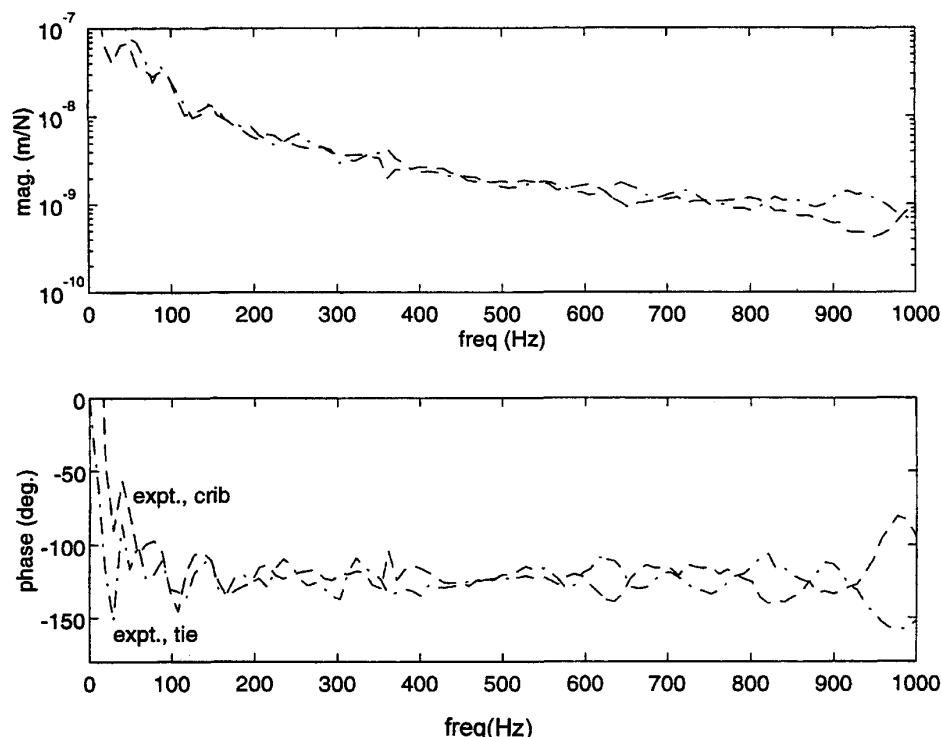


Figure B-3 Measurement vertical track receptance-RTD Site 2 (Wood in ballast, unloaded)

### CONCRETE TIE BALLASTED TRACK

Two sites with concrete tie ballasted track were measured—one at MTA and the other at BART. As a vehicle was not available to load the track, the ballast stiffness and damping in particular are probably not representative of those under a vehicle. Figure B-4 provides a comparison of the track model and experimental receptance for this case and Table B-3 shows the track characteristics.

### BOOTED TIE TRACK

Only one example of a booted tie system was encountered (at MTA) during the track measurements. Figure B-5 shows a comparison of the track model and experimental

receptance for this site. Table B-4 provides the track characteristics extracted from the model.

### EMBEDDED RAIL

Embedded rails are usually only found on light rail or streetcar systems. The only system of this type visited was RTD. The track construction is actually wood tie track with asphalt laid over the track up to the height of the railhead. One example of this type of track was measured and Figure B-6 shows the measured track receptance compared with the track model. Table B-5 shows the track characteristics. The tie spacing is not known because the ties are not visible. However, for the purposes of the analysis, the ties are presumed to be at the same 0.61-m spacing as the other wood tie track at RTD.

TABLE B-3 Concrete tie ballasted track characteristics

		Pad Stiffness	Pad Damping	Ballast Stiffness (per rail seat)	Ballast Damping (per rail seat)	Tie Spacing
Property	Site	(MN/m)	(kN.sec/m)	(MN/m)	(kN.sec/m)	(m)
BART	3	100	85	50	64	0.76

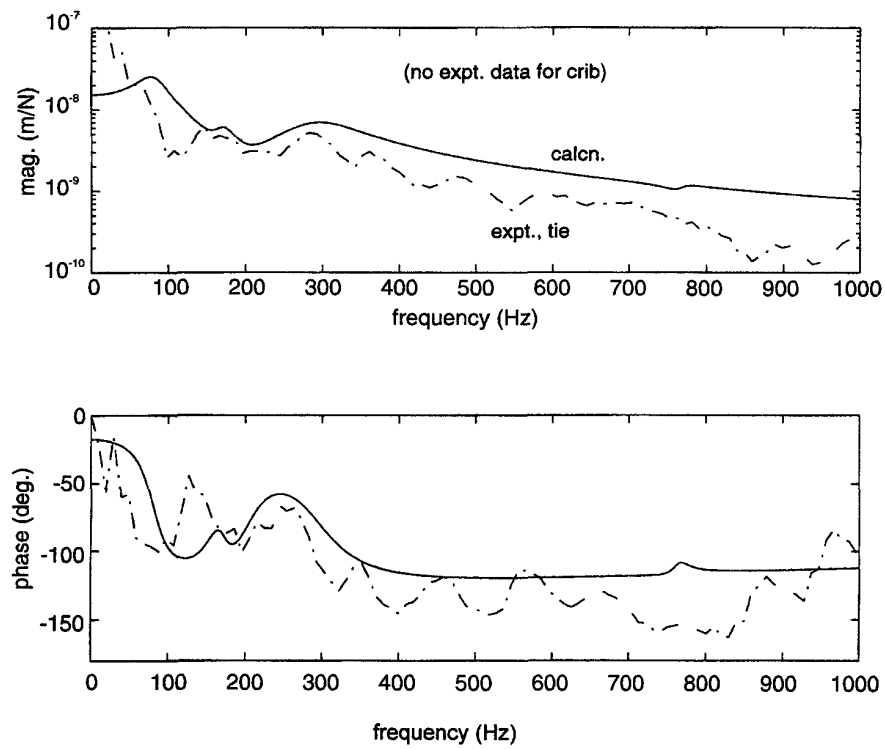


Figure B-4 Measured vertical track receptance-BART Site 3.

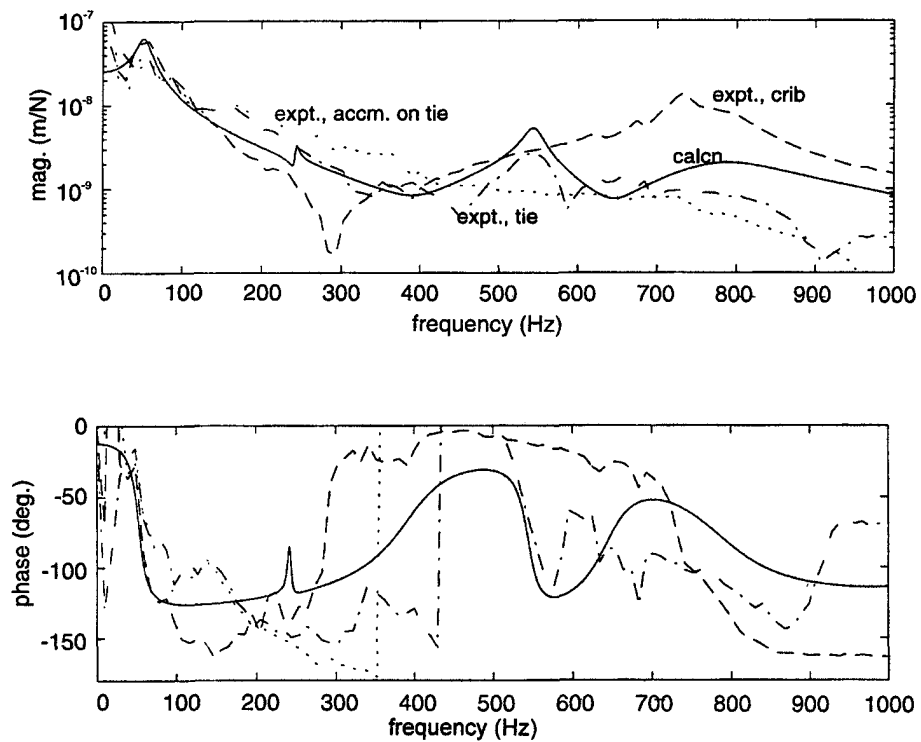


Figure B-5 Measured vertical track receptance-MTA Site 3

TABLE B-4 Booted tie track characteristics

		Pad Stiffness	Pad Damping	Boot Stiffness (per rail seat)	Boot Damping (per rail seat)	Tie Spacing
Property	Site	(MN/m)	(kN.sec/m)	(MN/m)	(kN.sec/m)	(m)
MTA	3	800	1300	20	19	0.76

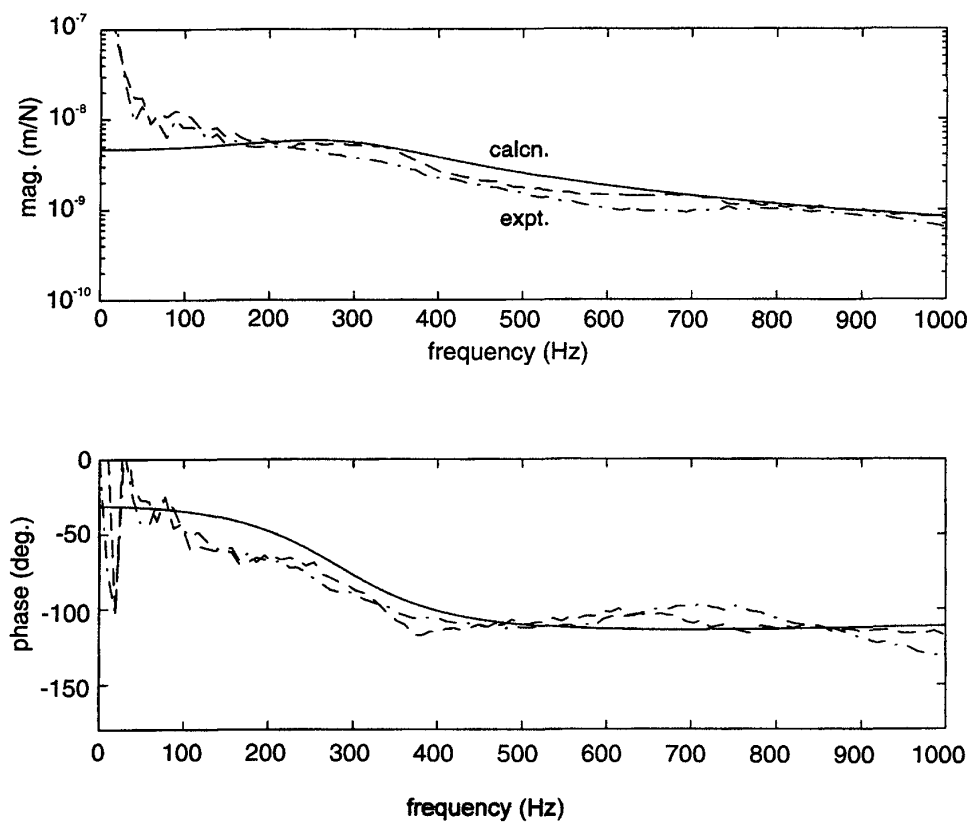


Figure B-6. Measured vertical track receptance--RTD Site 3.

TABLE B-5 Embedded track characteristics

		Ballast Stiffness (per rail seat)	Ballast Damping (per rail seat)	Tie Spacing
Property	Site	(MN/m)	(kN.sec/m)	(m)
RTD	3	92	59	0.61

## APPENDIX C

### WHEEL SET TEST AND MODELING RESULTS

Results are presented for all of the systems except WMATA. The wheel set receptance data gathered at WMATA were found to be corrupted with electrical noise at 60 Hz and a multitude of harmonics. As a result, no meaningful wheel set receptances could be extracted.

### TORSIONAL EXCITATION

The predicted receptance from the heavy rail wheel set torsional model to longitudinal excitation at the rim is shown in Figure C-1. The model results show a fundamental torsion mode at about 80 Hz and a second torsion mode at 300 Hz (Figure C-2). In the fundamental mode, the two wheels are rotating in antiphase; in the 300 Hz mode, the two wheels rotate in phase.

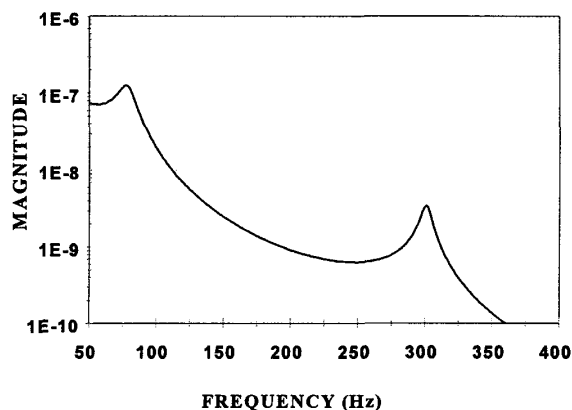


Figure C-1. Predicted powered wheel set torsional response.

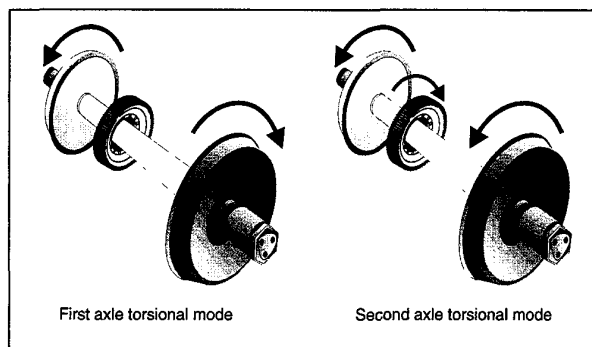


Figure C-2. First two torsional modes of powered wheel sets.

Figure C-3 shows a typical measured wheel set torsional receptance for the heavy rail vehicles. This particular result is from BART. However, results obtained from CTA and MTA also showed a second wheel set torsional mode in the 300- to 350-Hz range as can be seen in Table C-1.

Figure C-4 illustrates the measured wheel torsional receptance for the RTD powered truck. The receptance for the unpowered truck is very similar.

### RADIAL EXCITATION

Radial wheel receptances were measured primarily to determine the effective mass of the wheel when excited in the radial direction. However, the axle bending mode was also excited. A typical radial wheel set receptance from one of the heavy rail vehicles is shown, along with a theoretical receptance, in Figure C-5.

This particular example is from BART and indicates an effective wheel mass of 250 kg in the frequency range of

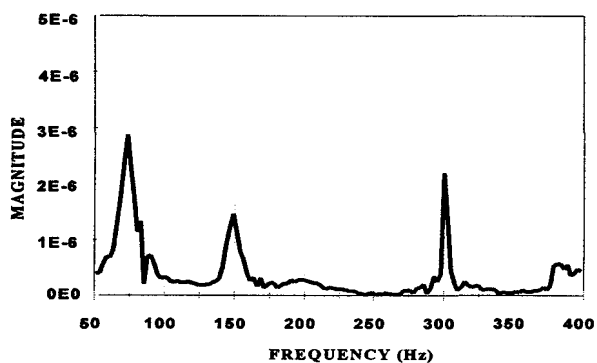


Figure C-3. Measured BART powered wheel set torsional response.

TABLE C-1. Wheel set torsional characteristics

	Effective Mass	Fundamental Torsional Frequency	Second Torsional Frequency
Property	(kg)	(Hz)	(Hz)
CTA	120	70	290
WMATA	n/a	n/a	n/a
MTA	150	70	350
BART	120	75	300
RTD	200	50	500

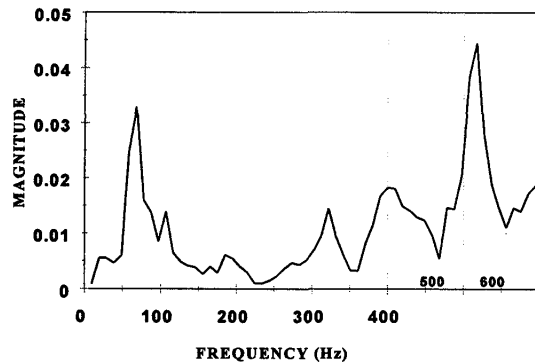


Figure C-4. RTD powered wheel set torsional response.

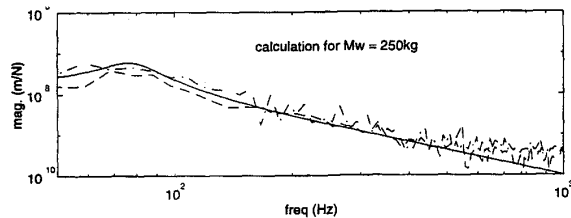


Figure C-5. Measured radial response of BART wheel set.

TABLE C-2 Wheel set radial characteristics

	Effective Mass	Fundamental Axle Bending Frequency
Property	(kg)	(Hz)
CTA	350	80
WMATA	n/a	n/a
MTA	150	70
BART	250	80
RTD	300	60

about 100 to 500 Hz, which is above the fundamental axle bending frequency of the wheel set at about 80 Hz. The mass of a single BART wheel is about 190 kg. So, in this frequency range, the effective mass is primarily that of the wheel.

The radial characteristics of the wheel sets at the various properties are shown in Table C-2. The truck arrangements in CTA and RTD incorporate an outboard axlebox with a chevron primary suspension, whereas the truck

arrangements at the other properties all have inboard bearings with a cylindrical rubber bushing forming the primary suspension. As a result, the wheel sets in CTA and RTD have higher effective radial wheel masses at high frequency than those at the other properties. The fundamental axle bending frequencies are very similar, except for RTD, which is somewhat lower as a result of a significantly smaller diameter axle. This is a direct result of the lower axle load of this light rail vehicle.

## LATERAL EXCITATION

Lateral excitation of the wheel set provided information primarily on the natural modes of the wheel plates. These modes have been discussed in detail by Grassie (1). He demonstrated that there are families of modes, which have combinations of nodal diameters and circles on the wheel plate. These mode shapes become ever more complex with increasing frequency (Figure C-6).

Figure C-7 shows a typical lateral receptance, which indicates three clearly defined modes in the frequency range

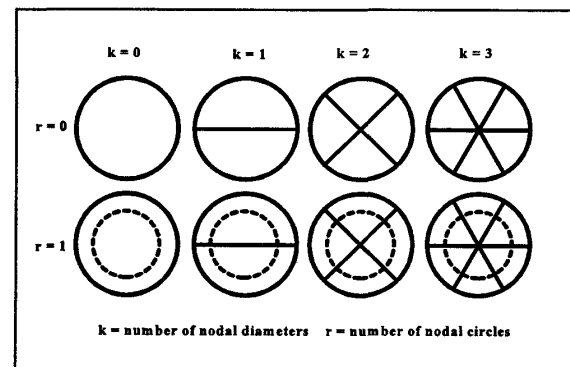


Figure C-6. Lateral Wheel set modes.

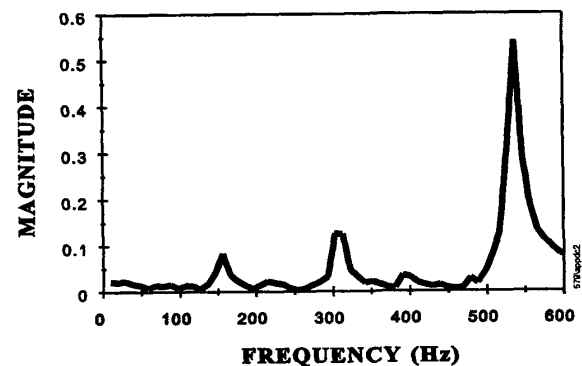


Figure C-7. Measured BART wheel set lateral response.

TABLE C-3 Heavy rail wheel set lateral characteristics

	1st Plate Lateral Frequency	2nd Plate Lateral Frequency	3rd Plate Lateral Frequency
Property	(Hz)	(Hz)	(Hz)
CTA	150	310	600
WMATA	n/a	n/a	n/a
MTA	220	400	680
BART	150	300	520

up to 600 Hz. The natural frequencies of the first three groups of wheel plate lateral modes that were apparent from the receptance tests at the heavy rail properties are presented in Table C-3.

RTD, once again produced significantly different results because of the resilient pads between the rim and hub of each wheel. In this case, no significant peaks were apparent in the lateral receptance until the 500- to 600-Hz frequency range.

## REFERENCES

1. Grassie, S. L. "Dynamic Modelling of Railway Track and Wheelsets," invited paper, Second International Conference on Recent Advances in Structural Dynamics, ISVR, University of Southampton, U.K., April 1984.

## APPENDIX D

### RESULTS FROM CORRUGATION INITIATION MODEL

This model was run to simulate corrugation formation for several cases with a representative heavy rail vehicle on both single- and double-layer track models. Both tangent track and curving situations were represented-with and without braking or traction torques applied to the wheel set.

The method of simulation that was used allowed the wheel set to initially reach a steady-state condition on smooth track. Subsequently, a rail surface irregularity in the form of a constant amplitude varying wavelength was introduced only on the right rail. The surface irregularities were introduced on one rail because there is no reason to expect any correlation between the initial surface roughness on the two rails. The range of wavelengths typically covered a frequency range up to about 400 Hz for the wheel set velocity being simulated.

Outputs from the program included time histories of

- Rail surface irregularity,
- Wheel and rail contact point vertical displacements, Wheel/rail normal force,
- Wheel rotational speed variation, and
- Wheel/rail wear.

These outputs were used to generate transfer function of all of the outputs relative to rail surface irregularity.

### VARIATION IN VERTICAL WHEEL/RAIL FORCE AND DISPLACEMENT

Figures D-1 and D-2 show, respectively, the wheel and rail contact point transfer functions relative to track irregularity for an example single-layer track. These show that, at very low frequency, the wheel follows the irregularity, and the rail does not displace. The well-defined single resonance that is apparent is the P2 resonance with the wheel and rail bouncing on the track stiffness. The frequency of this peak

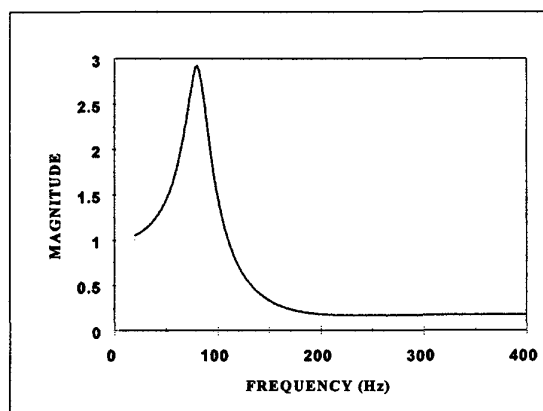


Figure D-1. Wheel displacement/irregularity transfer function--single-layer track.



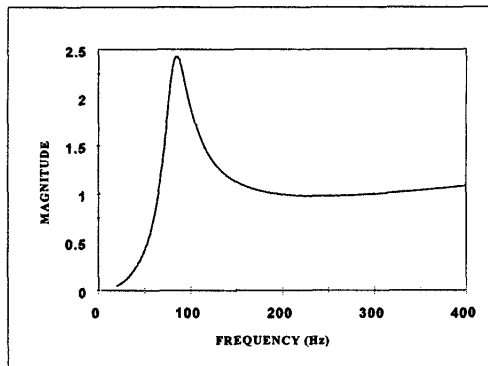


Figure D-2. Rail displacement/irregularity transfer function--single-layer track.

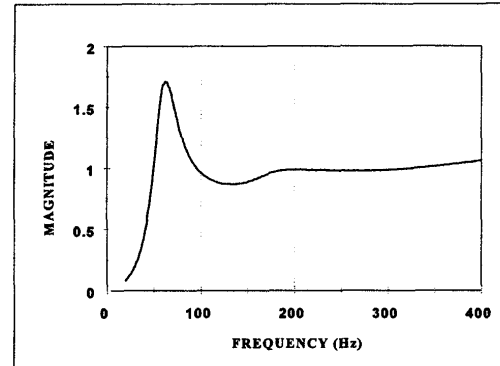


Figure D-4. Wheel displacement/irregularity transfer function--two-layer track.

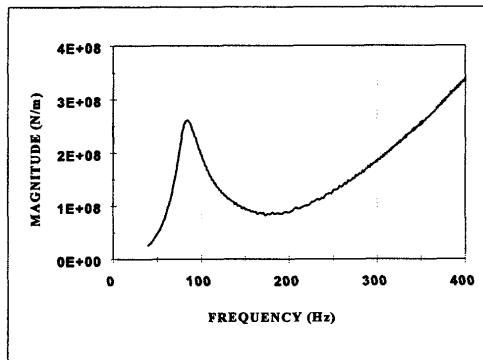


Figure D-3. Wheel/rail normal force/irregularity transfer function--single-layer track.

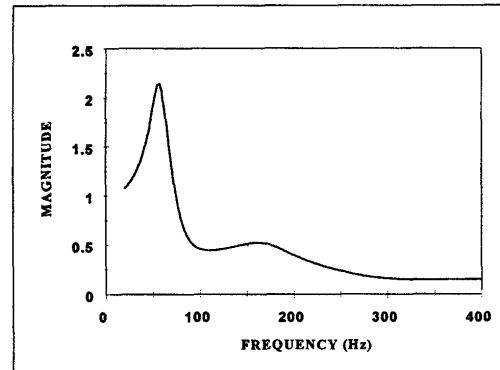


Figure D-5. Rail displacement/irregularity transfer function--two-layer track.

depends primarily on the wheel unsprung mass and the pad or ballast stiffness. Either decreasing the unsprung mass or increasing the support stiffness would increase the frequency of this mode. Above this resonance, the wheel displacement becomes progressively smaller and almost all of the irregularity amplitude is absorbed by rail deflection.

Figure D-3 illustrates the transfer function between rail irregularity and wheel/rail normal force. The amplitude of the peak is controlled by the unsprung mass and the track support stiffness and damping.

Figures D-4 and D-5 show, respectively, the wheel and rail contact point displacement transfer functions relative to rail irregularity for two-layer track. These figures show the same basic characteristics as those described previously for

single-layer track. However, in this case, two peaks are apparent; the lower frequency peak is the P2 resonance of the wheel bouncing on the ballast stiffness, and the upper peak is actually associated with an anti-resonance of the track, wherein the ties are bouncing vertically with a much larger amplitude than the rail.

Figure D-6 illustrates the transfer function of wheel/rail normal force to rail irregularity for the two layer track. Two peaks are apparent in this figure. The lower frequency peak associated with the P2 resonance is much smaller than the higher frequency peak, which is associated with the antiresonance described previously. This higher frequency peak can only be present with a two layer track system, such as concrete-tie ballasted track or booted-tie track.

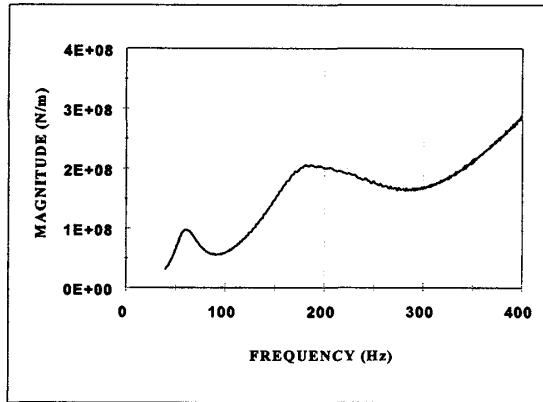


Figure D-6. Wheel/rail normal force/irregularity transfer function--two-layer track.

#### VARIATION IN WHEEL SET ROTATIONAL VELOCITY

The right wheel runs over the vertical irregularities in the rail surface with a longitudinal force acting on it because of the tractive effort. Variations in wheel/rail normal force occur as shown in Figure D-4. As a result, the right wheel rotational speed fluctuates in order to maintain a nearly constant longitudinal force in the presence of the fluctuating normal wheel force. The left wheel rotational speed also fluctuates as a result of the torque variations in the axle.

Figure D-7 shows the transfer function of the two wheel rotational speeds with respect to rail irregularity for direct fixation track. It can be seen that at the P2 frequency, which is near 100 Hz, there are large fluctuations in rotational speed on the right wheel but much smaller variations in rotational speed on the left wheel. However, at about 300 Hz, which is the frequency of the second wheel set torsional mode, there is a clearly defined peak in the rotational speed of the left hand wheel with no similar peak on the right hand wheel. The left-hand wheel, which is the one in contact with the rail without the surface irregularities, is acting as a vibration absorber.

#### VARIATIONS IN RAIL WEAR

The wheel rotational speed variations that were discussed in the previous section result in fluctuations in the longitudinal slippage or creepage between wheel and rail. This, in turn, causes variations in the surface wear of the rail. Previous work (1, 2) has shown that, because of the tangential creep forces at the wheel rail interface, wheel and

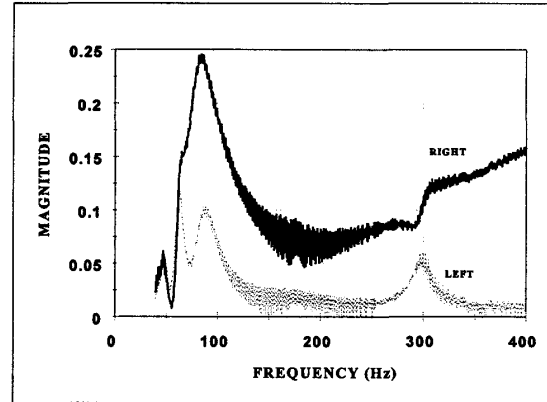


Figure D-7. Wheel rotational speed/irregularity transfer function--single-layer track.

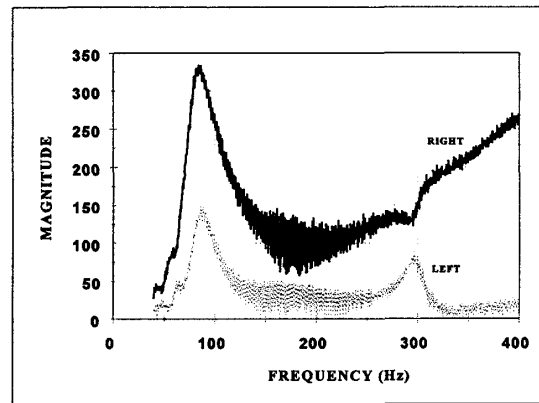


Figure D-8. Magnitude of wheel wear/irregularity transfer function--single-layer track.

rail wear are proportional to the work done. Work done per unit distance traveled along the track is equal to the sum of the longitudinal force multiplied by the longitudinal slippage and the lateral force multiplied by the lateral slippage.

In this particular case, each wheel is subject primarily to longitudinal forces due to tractive effort or to steering forces in curves. Accordingly, contributions to rail surface wear come almost entirely from longitudinal slippage. Figure D-8 shows the magnitude of the transfer function of wheel wear with respect to track irregularity.

Figure D-9 indicates the real part of the right wheel wear to track irregularity transfer function. When the real

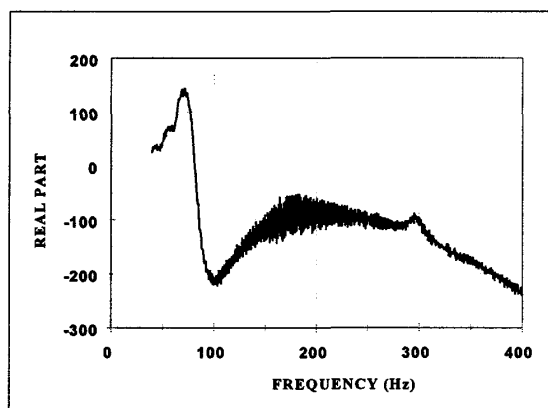


Figure D-9. Real part of right wheel wear/track irregularity transfer function--single-layer track.

part of this transfer function is negative, at that frequency the peaks in the wear occur at the locations of the troughs in the surface irregularity. This situation would cause irregularities at that frequency or wavelength to increase in depth and, therefore, grow out of the initial random distribution of surface irregularities. For the right wheel there is a negative peak at about 100 Hz but no clear peak in the vicinity of 300 Hz.

On the left wheel, however, Figure D-8 shows a peak at around 300 Hz in the magnitude of the wheel wear to track irregularity transfer function. This indicates that corrugations at that frequency are likely to develop on one rail as a result of surface irregularities on the other rail. In this case, the phase relationship of the transfer function is not important because the wear pattern that results is not reinforcing the surface irregularities already present on the rail.

## REFERENCES

1. Bolton, P.J., Clayton, P., and McEwan, I.J., "Wear of Rail and Tyre Steels Under Rolling/Sliding Conditions," Proc. ASME/ASLE Conference, San Francisco, CA, August 1980.
2. Clayton, P., Allery, M. B. P., and Bolton, P.J., "Surface Damage Phenomenon in Rails," Proc of Contact Mechanics and Wear of Rail/Wheel Systems, Vancouver, Canada, July 1982.

## APPENDIX E

### SUGGESTED CORRUGATION MITIGATION MEASURES

#### TREATMENTS PERTAINING TO THE TRACK

##### Treatments for Existing or New Track

The most severe type of corrugation is associated with the P2 resonance, in which the vehicle's unsprung mass moves on the resilience of the track form. This type of corrugation was observed only at Site 1 at BART, which had the stiffest type of direct fixation fastener of any of the five transit properties (i.e., 61 MN/m per rail seat with rail seats at 0.76-m spacing), whereas the next highest fastener stiffness was about 30MN/m. This high stiffness gives rise to a high vertical dynamic contact force and thus an increased propensity to form corrugation at the corresponding frequency. By inserting a 10-mm-thick, high-quality, studded rubber rail pad between the rail pad and the base plate, with an effective vertical dynamic stiffness of 60MN/m, it would be possible to reduce the effective vertical stiffness from 60MN/m to the level of about 30MN/m which appears, from circumstantial evidence, to be sufficient to prevent P2-type corrugations from forming. Rail pads of this stiffness are available commercially. A useful experiment would accordingly be to grind the existing corrugated rails over a length of a few hundred meters; replace the rail pads with sufficiently resilient rail pads over a length of roughly 100 m; then monitor the development of corrugation over both the test length with resilient rail pads and a contiguous length of track with the standard pads. Tassilly and Vincent (1, 2) have associated long wavelength corrugation on the Paris RATP with the resonance and installed resilient rail pads on track with concrete biblock ties as a successful means of reducing the rate of corrugation formation.

It would also be possible to reduce the stiffness of track such as that at BART by installing completely new base plate assemblies, but it is assumed here that the cost of doing this would be unattractive to a railway company for existing track, particularly if it were possible to modify the existing fastening assemblies satisfactorily. However, for new or rebuilt track, designers should note that relatively stiff, low damping, direct fixation fastening systems are associated with relatively severe, Type 1 corrugation. For track forms with 115RE rail and a 0.76-m fastening spacing, a fastening stiffness of 30MN/m or less and an effective viscous damping constant of 7.4kNs/m or greater appear to be sufficient to avoid this type of corrugation.

There is evidence from the work of both Tassilly and Vincent (1, 2) and of Ahlbeck et al (3) that resilient rail pads were a critical factor in alleviating the development of corrugation associated with the resonance of booted ties (i.e.,

Type 4 corrugation). There is also good reason to believe that, because resilient rail pads reduce vertical dynamic loading, they would also alleviate all types of corrugation whose development is exacerbated by vertical dynamic loading (e.g., corrugation arising from the pinned-pinned resonance/ anti-resonance [Type 5 corrugation]).

A treatment which has been demonstrably successful in reducing corrugation on the low rail in curves is to lubricate the gage face of the high rail. Indeed, this treatment is probably the singular most effective and most widely adopted treatment of corrugation in curves. Not only has its effectiveness been documented (1, 2, 3), but also the authors are aware of work which has demonstrated significant reduction in corrugation in the S-Bahn system in Copenhagen and in an underground tramway in Tokyo largely as a result of providing adequate high rail lubrication. Although the reasons why this treatment is effective are not entirely clear, the effectiveness of gage face lubrication has been demonstrated sufficiently compelling in practice for it to be plain that further examination of the reasons is required. One possibility is that lubricant on the gage face is carried over onto the railhead, with a consequent reduction in railhead friction.

The damage mechanism for all types of corrugation described here is wear, with the areas which become corrugation troughs worn more rapidly than the peaks. Because the wear rate can be reduced significantly using head-hardened rails, the adoption of such rails should, ipso facto, reduce corrugation formation. It would be expensive and difficult commercially to justify premature replacement of rails, even in corrugation-prone areas, with head-hardened rails. However, if the rails are to be replaced in such areas during routine maintenance, it is highly likely that their replacement with head-hardened rails would be cost-effective in view of the small premium in the cost of such rails. Headhardened rails have been installed in some curves of the S-Bahn system in Copenhagen and have brought sufficient reduction in the rate of corrugation formation for the railway system to believe that this is a useful treatment. It would certainly be advisable to install head-hardened rails in curves: on the low rail these will reduce the rate of corrugation formation, while in the high rail they will bring about a reduction in wear.

For Site 2 at BART, a very pronounced corrugation occurred which was associated with lateral resonance of the wheel set. This was apparently excited in some fashion by the presence of a guard rail, whereas at an adjacent site where there was no guard rail and only a slightly greater curve radius, there was no such pronounced corrugation. It would accordingly be reasonable to remove the guard rail from Site 2, grind through the site to remove existing corrugation, and then monitor the track periodically to determine whether the severe corrugation recurred or whether a different, less pronounced type of corrugation occurred.

There are two further treatments which should alleviate corrugation in the longer term. The first of these is the use of

a substance to control the coefficient of friction between wheel and rail. The particular modifications of frictional behavior which are desirable are that friction should increase with relative sliding between wheel and rail, thereby removing the possibility of stick-slip oscillations, and that the coefficient of friction should not be too great. The maximum value of the coefficient of friction in dry tunnels can approach 0.6, which gives extremely high values of tangential traction. In such circumstances, only a relatively low vertical load can be carried by the rail before this shears plastically, with the result that damage occurs very quickly. Typically the braking system of a vehicle requires only that the coefficient of friction be about 0.3, so there are attractions in using a friction modifier on the wheel tread to limit the coefficient of friction to about this value. It has been reported that use of such a commercially available friction modifier applied to the wheel tread has been a critical component of the treatment of corrugation on the Vancouver Skytrain system—largely, it is believed, because stick-slip was eliminated (4).

A treatment which has not been tested to date is asymmetric, profile grinding in curves. This would work by improving the steering of vehicles, reducing the curving forces required by the vehicle and thus also the tangential forces involved in slip, wear, and corrugation formation. No examples of asymmetric profile grinding to alleviate corrugation in curves have been reported in the literature. Reprofileing to influence conformity and local contact stresses has, however, been one component of successful treatment of corrugation on the Vancouver Skytrain system (4).

The status of the various treatments discussed in this section is summarized in Table E-1, which lists the treatments and their application or effectiveness (known or likely) to the alleviation of the five types of corrugation identified as occurring on North American transit systems. Some liberty has been taken here insofar as the categorization of corrugation advanced here is novel. Accordingly, although it may be known that a treatment has been successfully used to alleviate corrugation, the particular type of corrugation alleviated may not be known with certainty. There is some doubt regarding the type of corrugation arising from the second torsional mode of the wheel sets (i.e., Type 2 corrugation) because this is the first publication in which this type of corrugation has been identified. Despite these doubts, the research team believes that the treatments summarized in Table E-1 are a correct representation of the state of the art.

## Measures for New Track

All of the recommendations that pertain to existing track apply also to new track. In particular, for the direct fixation track form, it is essential to have a relatively low dynamic stiffness in order to avoid corrugation arising from the P2

TABLE E-1 Treatments of corrugation involving changes to track form

	Treatment	Type of Corrugation				
		1	2	3	4	5
1.1	Resilient DF fastener	++	-	-	-	+
1.2	Resilient railpad	+	+	-	+	+
1.3	High rail gage face lubrication	-	++	-	++	-
1.4	Control railhead friction	+	+	+	+	+
1.5	Head-hardened rail	++	++	+	+	+
1.6	Remove guard rail	-	-	+	-	-
1.7	Asymmetric profile grinding	-	+	+	+	-
1.8	Limit curve radius (to 400m)	-	+	+	+	-
1.9	Limit traction and braking	+	+	-	-	-
1.10	Irregular fastener spacing	-	-	-	-	+

Notes: ++ = currently used successfully on one or more transit systems

+ = likely to be successful, but not yet tested

- = no recommendation

resonance (Table E- 1). In addition, there should be adequate lubrication in curves, and the use of head-hardened rail should be considered, if not throughout the system, then at least in curves, particularly if the radius is less than 400 m. Indeed, given that 400 m appears to be a critical radius, below which corrugation is very much more likely to occur, it would be desirable to regard this as a sensible limit on curve radius in order to limit the severity of corrugation. Clearly, however, there are more concerns than corrugation when constructing new track.

Corrugation is evidently more severe wherever traction is required (i.e., locations where trains start and stop [e.g., stations and signals] and grades up or downhill). The experience of severe corrugation formation on CTA, where there are relatively high traction and braking rates (a maximum of about 4.5km/h/s), suggests that it would be advisable to limit these to more conventional values. As with the curve radius, there are more concerns in building a railway than limiting corrugation formation, but it may nevertheless be helpful for track designers at least to be aware of these factors.

The corrugation associated with the track's pinned/pinned resonance/anti-resonance (i.e., Type 5) could, in principle, be alleviated by reducing the effect of this resonance. One means of doing this is to use resilient rail pads between rail and the tie or base plate. Another means of doing so would be to build the track with slightly irregular tie or fastener spacings. Although possible in principle, this is unlikely to be attractive in practice.

## TREATMENTS PERTAINING TO VEHICLES

### Treatments for Existing Vehicles

Whereas there are many treatments involving modification

to the track form for corrugation on existing track, there are relatively involving modifications to existing vehicles. Two such treatments are simply the analogue of track form-oriented treatments: modification of frictional conditions on the wheel tread and on the flange. The effectiveness of these measures for attenuating corrugation of Type 5 has been demonstrated on the Vancouver Skytrain system (4). These treatments are summarized in Table E-2.

This project has revealed a novel treatment which could be made to existing vehicles: the adoption of a torsional vibration absorber tuned to the second torsional resonance of driven wheel sets. In view of the paucity of vehicle-oriented corrugation treatments and also of the evident prominence of the second torsional mode in formation of corrugation on transit track, the use of a torsional vibration absorber, in principle, holds tremendous promise. If it were demonstrated that a torsional vibration absorber could indeed greatly mitigate corrugation formation and if it were possible to develop such an absorber (which could be made and installed at sufficiently modest cost), this could be part of a satisfactory treatment of the corrugation problem on U. S. transit track.

### Treatments for New Vehicles

In a new vehicle, the same measures can be taken to alleviate corrugation as have been suggested for existing vehicles. In addition, other modifications could, in principle, be made. Those which offer greatest promise of success at relatively little cost are the following:

- The use of resilient wheels to modify wheel set resonances, particularly the torsional modes associated with Type 2 corrugation and the lateral modes associated

**TABLE E-2 Treatments of corrugation involving changes to vehicles**

	Treatment	Type of Corrugation				
		1	2	3	4	5
2.1	Wheel flange lubrication	-	+	-	+	-
2.2	Control wheel tread friction	+	+	+	+	++
2.3	Torsional vibration absorber	-	+	-	-	-
2.4	Improve steering	+	+	-	+	-
2.5	Resilient wheel sets	+	+	+	+	+
2.6	Resilient drive	-	+	-	-	-

Notes: ++ = currently used successfully on one or more transit systems

+ = likely to be successful, but not yet tested

- = no recommendation

with Type 3 corrugation. More generally, resilient wheel sets offer a means of reducing the effective unsprung mass, thus reducing the probability of forming corrugation by excitation of the P2 resonance.

- The adoption of a resilient drive arrangement, thus decoupling the traction motor dynamically from the axle and reducing the propensity to form Type 2 corrugation.
- Improved steering of bogies, thus facilitating negotiation of curves and reducing traction at the wheel/rail contact.

So far as is known to the research team, no railway system has adopted any of these measures specifically to alleviate corrugation. However, based on the evidence of an absence of severe corrugation at RTD, there is good reason to believe that a resilient drive and resilient wheel sets would alleviate corrugation significantly.

## CONCLUSIONS

Various treatments of corrugation have been identified which could be implemented by making changes to either the track or the vehicles. Whereas most track-form-oriented treatments could be adopted on existing track, most treatments involving changes to vehicles could be implemented satisfactorily only on new vehicles. The principal exception to this is the novel treatment proposed by the research team of attaching a tuned torsional dynamic vibration absorber to the driven axles of a vehicle. The principal objective of such an absorber would be to attenuate and give damping in the second torsional mode of the wheel sets.

Most track-form-oriented changes have been implemented by transit systems interested in reducing the costs of corrugation mitigation by regular maintenance grinding; however, very little information is available regarding the costs and benefits of these changes. Nevertheless, some changes made by one or more transit systems show promise. Considerable research would be required in order to under-

take a full-scale cost-benefit analysis. Appendix F gives a brief overview of a simple economic analysis.

## REFERENCES

1. Tassilly, E. and Vincent, N., "Rail Corrugations: Analytical Model AND Field Tests," *Wear*, 1991, 144, p.163-178.
2. Tassilly, E. and Vincent, N., "A Linear Model for the Corrugation of Rails," *Jnl of Sound and Vibration*, 1991, 150, p.25-45.
3. Ahlbeck, D.R., and Daniels, L.E., "Investigation of Rail Corrugations on the Baltimore Metro," *Wear*, 1991, 144, pp. 197-210.
4. Kalousek, J. and Johnson, K.L., "An Investigation of Short Pitch Wheel and Rail Corrugation on the Vancouver Skytrain Mass Transit System," *Proc of Instn Mech Engrs.*, 1992, 206F, pp.127-135.

## APPENDIX F

### SIMPLE ECONOMIC ANALYSIS OF POTENTIAL CORRUGATION MITIGATION MEASURES

Tables F-1, F-2 and F-3 present relative annual cost comparisons for various corrugation mitigation measures as their costs relate to grinding as the base case measure for corrugation control. Table F-1 refers to measures for existing track, Table F-2 refers to measures for new track, and Table F-3 refers to measures for vehicles. Because such costs are inherently specific to individual route designs, track designs, mechanical equipment specifications, and systems operations, these comparisons only offer an "order-of-magnitude" assessment of the various methods. In addition, the cost orders of magnitude presented here apply to corrugation-prone track only.

Following the tabulated data are the assumptions used in determining the economics of the mitigation measures.

TABLE F-1 Measures for existing track

<b>Treatment Method</b>	<b>Cost Relative to Rail Grinding</b>
Asymmetric Profile Grinding	1.0
Resilient Rail pad - Direct Fixation Track	11.3
Resilient Rail pad - Ballasted Track	31.3
High Rail Gauge Face Lubrication	0.5
Control Railhead Friction	-1.8
Head Hardened Rail	-2.0
Remove Guard Rail	2.9
Limit Traction and Braking	Design Specific

TABLE F-2 Measures for new track

<b>Treatment Method</b>	<b>Cost Relative to Rail Grinding</b>
Resilient Rail pad - Direct Fixation Track	0
Resilient Rail pad - Ballasted Track	0
Head Hardened Rail	-2.0
Limit Curve Radius (to 400m)	Design Specific
Irregular Fastener Spacing	Design Specific

TABLE F-3 Measures for vehicles

<b>Treatment Method</b>	<b>Cost Relative to Rail Grinding</b>
Wheel Flange Lubrication	0.5
Control Wheel Tread Friction	-1.8
Torsional Vibration Absorber	?
Improve Steering	Design Specific
Resilient Wheel sets	?
Resilient Drive	?

## ASSUMPTIONS USED IN DETERMINING THE ECONOMICS OF THE MITIGATION MEASURES

### General

1. Assume a system of 200 track miles
2. Assume 5 percent of the system (10 track miles) is subject to corrugation problems.
3. Assume 100 vehicles operating at a capacity of 100,000 miles/year.
4. Assume 4 axles per vehicle.
5. Any initial costs are annualized over a 10-year period at 10 percent after tax cost of capital.
6. Any benefits (such as reduced wheel or rail wear) associated with applying a technology to prevent corrugations are credited back to the cost of implementation

### Profile Grinding

1. Profile rail grinding costs are approximately \$1480/passmile
2. Profile rail grinding averages 2.5 pass-miles per track mile per trip.
3. Profile rail grinding is required approximately 1 time per year.
4. In this application, rail grinding effects are negligible with respect to normal wear in terms of rail replacement requirements.

### Resilient Rail Pad Replacement - Direct Fixation Track

1. Cost per rail seat is \$55.00 for direct fixation track.
2. Two rail seats per track fixation.
3. Track is on 30" fixation centers.
4. Labor for fixation assembly is 15 minutes per fixation. 5 Labor cost per hour is \$20.00 and includes fringe benefits.

### Resilient Rail Pad Replacement - Concrete Ties, Full Pad/Plate Replacement

1. Top pad cost is \$2.00 per pad.
2. Plate and bonded pad assembly (lower pad) cost is \$75.00 per plate/pad.
3. Two plate/pad assemblies per tie.
4. Fasteners cost \$70.00 per fastener assembly
5. Tie spacing is 30"
6. Labor and capital equipment costs for this type of work are essentially the same as the labor and capital requirements required to relay rail which is estimated at \$90,000 per track mile.

### Wayside High Rail Gage Face Lubrication

1. Hydraulic wayside lubricator purchase, installation, ownership and operating cost is \$2,000 per year per lubricator.
2. Hydraulic wayside lubricator spacing is approximately 1 lubricator per track mile where installed

### Control Railhead Friction by Friction Modifier Application

1. Railhead friction modifier installation costs are approximately \$1750 per vehicle.
2. Railhead friction modifier operating costs are approximately \$180 per month per vehicle operating at 62,000 miles/year.
3. Railhead friction modifier application units are required on 25 percent of the axles within a train set.
4. Wheel life is increased by a factor of 2 on lubricated track due to reduced wear on wheels from the use of friction modifier.
5. Track is assumed to be appropriately lubricated.
6. Wheel replacement costs are \$6,000 per vehicle.
7. Wheel replacement is required once every 3 years without use of friction modifier.

### Head-Hardened Rail

1. Rail laying capital cost other than for rail is \$90,000/track-mile.
2. Premium rail costs \$590/ton.
3. Standard rail costs \$500/ton.
4. Rail in transit applications averages 115 lb/yd.
5. Replacement cycle for standard rail is 5 years.
6. Replacement cycle for premium rail is 7 years

### Remove Guard Rail

1. Guard rail removal costs are \$100 per foot.
2. Hydraulic wayside lubricator purchase, installation, ownership and operating costs is \$2,000 per year per lubricator.
3. Hydraulic wayside lubricator spacing is approximately 1 lubricator per track mile where installed.

### Wheel Flange Lubrication

1. Same as High Rail Gauge Face Lubrication

### Control Wheel Tread Friction

1. Same as Control Railhead Friction

The benefits of those techniques with negative cost factors reap benefits in addition to corrugation mitigation. Those with very large cost factors, such as those related to rail pads, should only be considered during programmed rail replacement.



Again, because of the unique characteristics of individual transit systems, the assumptions were made in order to provide a generic assessment of cost orders of magnitude. The sources of the assumptions vary from surveys of railway equipment suppliers, surveys of railway maintenance contractors, surveys of individual railroads, and documented industry experience to professional/technical judgment. As can be expected, the costs and efficacy of individual products or techniques varies depending on whom one speaks with. In such cases, compromises are made in an attempt to develop reasonable assumptions without bias to any one railway company or supplier.

Individual mitigation measures require either initial costs, periodic costs, incremental costs, non-periodic interim costs, or all of the above. To provide an "annual cost" assessment, the following conventions apply:

- Annual costs are steady with no increases as a result of inflation.
- Periodic and irregular costs that do not occur annually are annualized using a 10-year time horizon and a 10percent discount rate.
- All initial investments are annualized using a 10-year time horizon and a 10-percent discount rate.
- Some mitigation measures provide alternate benefits in addition to the mitigation of corrugations. Examples are the use of friction modifiers that could reduce wheel wear and the installation of head-hardened premium rail that could reduce rail wear. In these cases, those benefits are credited back to the implementation costs, which, in some cases, generates a negative order-of magnitude comparison. What this indicates is that the application of that technology could mitigate the corrugation and save the transit system money in other areas of operations and maintenance.

- Several of the mitigation measures are too design-specific to be able to assess the cost of order-of-magnitude data within any reasonable degree. These measures are indicated in the following tables with the words "design-specific." In addition, some of the measures cannot be economically assessed until further work is carried out. These measures are indicated in the tables with a question mark.
- This analysis assumes that by applying the individual mitigation measures, the need for grinding corrugations is eliminated altogether. For some, or all, measures, this may not be a realistic assumption. Again, the implementation characteristics are so highly situation specific that individual analyses would be necessary prior to making any final business decision regarding a mitigation technique.

This analysis provides only an order-of-magnitude cost comparison for the various mitigation techniques. The same analysis considering the many unique factors of individual systems would probably yield a wide variation of cost comparison differences. It would be imprudent for any transit system to make final decisions based on simply multiplying the cost magnitude of any mitigation measure by a company's cost of grinding to control corrugations. These data are useful to identify those measures worthy of further consideration for the control or mitigation of rail corrugations.

It is strongly recommended that a detailed and comprehensive study be performed to assess the economics of these mitigation measures as they pertain to specific systems and types of corrugations. Such a study would need to include detailed economic information specific to individual transit systems, mechanical equipment specifications, track structures and designs, and operating scenarios.